Long-Term Trends in Water Quality Parameters in Coastal Waters of Puerto Rico

By

Ali Amirrezvani

A thesis submitted in partial fulfillment of the requirements for the degree of

MASTER OF SCIENCES
in
MARINE SCIENCES
(BIOLOGICAL OCEANOGRAPHY)

THE UNIVERSITY OF PUERTO RICO
MAYAGÜEZ CAMPUS
2016

Approved by:

Roy A. Armstrong, Ph.D. — Date
President, Graduate Committee

Jorge R. García-Saís, Ph.D. — Date
Member, Graduate Committee

Fernando Gilbes-Santaella, Ph.D. — Date
Member, Graduate Committee

Yasmín Detrés, Ph.D. — Date
Member, Graduate Committee

Karen Ríos, Ph.D. — Date
Representative of Graduate Studies

Ernesto Otero-Morales, Ph.D. — Date
Chairperson of the Department of Marine Sciences

ABSTRACT

Ocean color remote sensing technology has been widely used in coastal water quality research. Of particular importance is the influence of river discharge on turbidity and chlorophyll concentration in coastal areas, which is seasonally and spatially variable. The coastlines and landscapes of Puerto Rico exhibit regional variability. In this study, Sea-Viewing Wide Field-of-View Sensor (SeaWiFS) and Moderate Imaging Spectroradiometer (MODIS) Aqua satellite chlorophyll *a* concentration ([Chla]) and diffuse attenuation coefficient at 490nm (Kd490) data, at high spatial resolution, in combination with river streamflow discharge from the United Stated Geological Survey (USGS) were used to assess long-term trends impacting the diverse (*i.e.*, Western, Northern, Eastern, and Southern) coastal waters along Puerto Rico for the years 1998 to 2013. The evaluation of Kd490, [Chla], river discharge time-series, and their correlation coefficients from 2km to 16km from the river mouth showed seasonal and spatial variation for the four regions of the island. Chlorophyll *a* concentration was the main contributor to turbidity in coastal waters of Puerto Rico during 1998 to 2013. Higher turbidity trends were primarily due to increased [Chla] (*i.e.*, biogenic particles) compared to inorganic sediments, as shown by the high correlation between Kd490 and [Chla], especially during the dry season, compared to the rainy season. Kd490 and [Chla] were not related to river discharge.

RESUMEN

La tecnología de percepción remota del color del océano ha sido ampliamente utilizada en la investigación de la calidad del agua costera. De particular importancia es la influencia de la descarga de los ríos sobre la turbidez y la concentración de clorofila en las zonas costeras, que es variable estacional y espacialmente. Las costas y paisajes de Puerto Rico muestran variabilidades regionales. En este estudio, la concentración de clorofila *a* ([Chla]) y del coeficiente de atenuación difusa a 490nm (Kd490), del sensor de campo de visión amplia de mar (SeaWiFS) y del espectroradiómetro de imagen moderada (MODIS) Aqua, con alta resolución espacial, en combinación con las medidas de descargas de ríos obtenidas por el Servicio Geológico de los Estados Unidos (USGS), se utilizaron para evaluar las tendencias a largo plazo que afectan las diversas aguas costeras (*i.e.*, Oeste, Norte, Este, y Sur) a lo largo de Puerto Rico para los años 1998 hasta 2013. La evaluación de las series de tiempo de Kd490, [Chla], y de descarga de los ríos, y sus coeficientes de correlación de 2km a 16km de la desembocadura de los ríos mostraron variación temporal y espacial para las cuatro regiones de la isla. La concentración de clorofila *a* fue el principal contribuyente a la turbidez en las aguas costeras de Puerto Rico durante 1998 a 2013. Las mayores tendencias de turbidez se debieron principalmente al aumento de [Chla] (*i.e.*, partículas biogénicas) en comparación con sedimentos inorgánicos, como lo demuestra la alta correlación entre Kd490 y [Chla], especialmente durante la época seca, en comparación con la época de lluvia. Kd490 y [Chla] no estaban relacionados con las descargas de los ríos.

Keywords: Chlorophyll *a* concentration, diffuse attenuation coefficient at 490nm, long-term trends, turbidity, river discharge, sediments, seasonal variation, regional heterogeneity, wind resuspension, shelf topography.

COPYRIGHT

Ali Amirrezvani
December 12, 2016

DEDICATION

To My Dear Family

ACKNOWLEDGMENTS

I would like to sincerely express my gratitude to Dr. Roy Armstrong, my advisor, for giving me the chance to research under his supervision and for his motivation and support during my studies. I would to thank the other members of my graduate committee, Drs. Jorge R. García-Saís, Fernando Gilbes-Santaella, and Yasmín Detrés, for their contribution to achieve my work.

I would to thank Drs. Nilda E. Aponte, John M. Kubaryk, and Ernesto Otero, for their support and valuable advice during my graduate education and master thesis duration.

I would like to thank Dr. Karen Ríos-Soto, for her constructive suggestions to complete my master thesis.

I would like to thank Drs. Stacey M. Williams and Juan J. Cruz Motta for expanding my knowledge in statistics and for advice in improving my research.

I would like to thank Dr. Sara Rivero, Dr. Aurora Justiniano, Dr. William J. Hernández-López, Ms. Myrna J. Santiago, Ms. Maria Cardona-Maldonado, Ms. Suhey Ortiz Rosa, and Ms. Cynthia Ramos, for their advice and moral support.

I would like to thank Aldo Acosta-Torres for his significant computer guidance and help.

I would like to thank Monserrate Casiano, Zulma Martinez, Lilivette Valle, Nilda E. Ramírez, and Jossie J. Moulier, for their very courteous administrative guidance and help.

I would to thank Luis Lugo for his guidance and help, and all around friendliness.

At last, but most important, I would like to thank my parents and my brother, for their unconditional support, inspiration and love.

And finally, I would like to thank my dog, for her pet assistance and support.

TABLE OF CONTENTS

LIST OF FIGURES

LIST OF TABLES

1 INTRODUCTION

In the first section of this study, the significance, statement, and causes the problem are discussed. Some background information about turbidity and chlorophyll concentration is included. Previous works on remote sensing of water quality parameters and their long-term trends are described. Regional settings of Puerto Rico in climate, river runoff, sediments, and shelf topography are also integrated.

1.1 Significance of the Study

Ocean color remote sensing technology has been widely used in coastal water quality research. There is a major influence of river discharge, turbidity, and chlorophyll concentration in coastal waters of Puerto Rico. Also, the coastlines and landscapes of Puerto Rico exhibit high regional variability.

1.2 Statement of the Problem

Sediment and turbidity are important ecological correlates, which influence the distribution of benthic communities. Suspended sediments, not only cause water column turbidity, but also result in lower light penetration. Associated nutrient inputs (*i.e.*, nitrogen and phosphorus) present in various forms (*i.e.*, nitrate, nitrite, ammonia, and organic) from river runoff cause eutrophication. Increased eutrophication results in algal blooms and possibly to other harmful blooms.

1.3 Causes of the Problem

Long-term rainfall chronic events determine regional and temporal trends in water quality parameters and influence the community structure of benthic communities. In addition, episodic events produce heavy rainfall and bring along runoff, sediment, and nutrient inputs.

1.4 Turbidity

Turbidity is an index of water quality. Several factors influenced turbidity, such as chlorophyll concentration (*i.e.*, phytoplankton), gelbstoff (*i.e.*, yellowish-brown acid material), and tripton (*i.e.*, inorganic matter) (Kirk, 2011). Turbidity reduces light penetration in the water column and it is directly proportional to river discharge. Resuspension of sediments from winter storm swells in the North and West regions is significant. Episodic events significantly influence turbidity patterns in coastal areas. As a result, the diffuse vertical attenuation coefficient for downward irradiance at 490nm (Kd490) was used as a proxy for turbidity.

1.5 Chlorophyll concentration

Chlorophyll *a* concentration ([Chla]) is the key light absorbing phytoplankton pigment in photosynthesis. Satellite ocean color data are used to estimate chlorophyll concentration. [Chla] is a proxy for phytoplankton biomass. Chlorophyll concentration is an indication of phytoplankton bloom and eutrophication. In addition, [Chla] drives primary production models at global scales. The euphotic (*i.e.*, sun light) zone in some shallow waters exhibits prominent productivity (Kirk, 2011).

1.6 Literature Review

1.6.1 Remote Sensing of Water Quality Parameters

The use of conventional, *in situ* methods for studying water quality parameters are inadequate to continuously characterize heterogeneous and patchy areas and are also costly and lengthy (Khorram *et al.*, 1991). The use of remotely sensed data provides a synoptic view compared to conventional methods and has been used to map and evaluate shallow coastal waters (Bierwirth, Lee, and Burne, 1993). The relationship between chlorophyll concentrations and suspended sediments and the patterns of near-shore discharges and distribution has also been studied using remote sensing (Fieldler and Laurs, 1990; Walker, 1996). Remote sensing provides significantly more information than ecological water quality modeling and *in situ* measurements on, for example, Secchi depth and chlorophyll *a* concentration (Dekker *et al.*, 1996). Remote sensing has been used to address insular shelf as well as estuarine sediment transport dynamics (Johnson and Harriss, 1980). Simultaneous acquisition of surface water quality samples and remote sensing data were found to be helpful in studies of phytoplankton biomass in coastal waters and estuaries in relation to spatial and seasonal variations (Catts *et al.*, 1985).

The evaluation of bio-optical relationships between space born ocean color and phytoplankton pigments started with the Coastal Zone Color Scanner (CZCS), which operated from 1978 to 1986 and generated phytoplankton pigment distribution maps (Gordon and Morel, 1983). SeaWiFS, launched in 1997, provided better spectral and radiometric resolution of the global ocean color field than CZCS (Hooker *et al.*, 1992). SeaWiFS provided data until 2010 and made it possible to generate near-real time global ocean color images (McClain *et al.*, 1998; O'Reilly *et al.*, 1998). SeaWiFS provided global ocean 2-day coverage and with 1km^2 nadir resolution. MODIS Aqua data are available since 2002 (Carder *et al.*, 1999; Esaias *et al.*, 1998). Ocean color data from SeaWiFS and MODIS provide estimates of chlorophyll *a* content in near surface waters (Miller and McKee, 2004).

The effects of land use on water quality in coastal waters have been studied by Miller and McKee (2004) using remote sensing and *in situ* measurements of chlorophyll and suspended sediments concentrations. Many studies have used remote sensing techniques to map total suspended matter (TSM). Nevertheless, there are limitations to the operational use of remote sensing techniques due to the lack of relatively high spatial and temporal resolutions required to observe coastal horizontal gradients. On the other hand, airborne systems improved spatial and temporal resolutions but are expensive to operate.

Remote sensing techniques in combination with numerical ocean circulation models and river discharge have been used to evaluate terrestrial runoff in Meso-American waters (Wilkinson, 1999). Results demonstrated that the Meso-American Barrier-Reef System (MBRS) reefs were seasonally controlled by terrestrial runoff with minimum values from March to April and maximum values from October to January (McKergow *et al.*, 2005).

Sheng *et al.* (2007) tracked the concentration of turbidity plumes after Hurricane Mitch made landfall in the MBRS in 1998 using SeaWiFS data. They found that terrestrial runoff could reach inshore reefs and atolls, and that river discharge seasonality controlled terrestrial runoff into the oceanic areas.

In Mayagüez Bay, Puerto Rico (Miller *et al.*, 1994) showed that light to moderate sediment river plumes discharge were restricted to near-shore regions, whereas, only during episodic high discharge events, the sediment plumes reached the reefs. In addition, SeaWiFS satellite data were used to show the evolution of chlorophyll *a* concentrations and Kd490 in coastal waters of the Puerto Rico shelf after Hurricane Georges (Gilbes *et al.*, 2001).

1.6.2 Long-Term Trends in Water Quality Parameters

In periods of strong storm-swells, the levels of resuspended sediments might have often surpassed 20 mg/l and even attained over 200 mg/l (Kleypas, 1996; Larcombe *et al.*, 1995). Similarly, terrestrial river runoff could have produced fluctuating concentrations of suspended sediments, which were greater than 10 and even exceeded 200 mg/l (Katwijk *et al.*, 1993; Kleypas, 1996; Miller and Cruise, 1995).

Large volumes of sediment-rich waters were transported to the coast and shelf after tropical storms and hurricanes passed over/near the Dominican Republic and generated vast runoff (Ahmad, Scatena, and Gupta, 1993; Gupta, 1988, 2000; Soler-López, 2001). Every ten to twenty years, a major hurricane passes over Puerto Rico (Ho, 1975; Neuman, Jarvinen, and Pike, 1990; Scatena and Larsen, 1991). In addition, substantial runoff transporting and eroding vast quantities of sediments to the coast are generated from winter frontal storms (*e.g.*, January 6, 1992; Torres-Sierra, 1996).

In Southwestern Puerto Rico, sedimentation occurs more in the inner and mid shelves compared to the shelf edge (Morelock *et al.*, 2001). Terrigenous material decreases from offshore so little runoff reaches the outer shelf resulting in more oligotrophic waters away from the coast. According to Ballantine *et al.* (2008) chlorophyll *a* concentration and turbidity decrease from inshore to offshore except during major storms, when it is closely associated with precipitation and runoff. In addition, sedimentation and nutrient runoff levels have increased over time. Water quality has deteriorated because of urban and industrial development as well as poor land use practices. Taken together, recent increase in cyanobacterial growth at shelf edge reefs might reflect high levels of nutrients (Ballantine *et al.*, 2008).

1.7 Regional Settings – Puerto Rico

Puerto Rico displays a moist warm climate accompanied with high relief mountains comprising 60% of the island area of 8711 km^2. It also exhibits variable coastlines and landscapes at regional scales. For instance, the North central margin has flat coastal plains. In the West coast, the turbidity of the water is less influenced by river discharges than by wind resuspension of bottom sediments during winter months (Warne, Webb, and Larsen, 2005).

The average rainfall in Puerto Rico during 1998 to 2013 was of 73.44 inches (*http://www.weather.gov/sju/averagerainfall*). The dry season period is from December to May. The rainy season is from June to November, in relation to the hurricane season in the Atlantic Ocean.

Some authors reported that agricultural erosion and soil erosion bring humic substances, minerals, nitrogen, phosphorus, and potassium on to the Puerto Rican shores, along with increasing sedimentation (Warne, Webb, and Larsen, 2005).

According to Abal and Dennison (1996), organic particles and fine clays easily resuspended from the sea floor, lowered light during long periods of time and at the same time went under resuspension and deposition cycles. Also, production of phytoplankton increased by augmented nutrient runoff into semi-enclosed seas, which also lowered light penetration and augmented turbidity (*op. cit.*). In the Western coast of Puerto Rico, light penetration increases from inshore to offshore, with more variability offshore (Gilbes, López, and Yoshioka, 1996).

According to Morelock *et al.* (2000), in Puerto Rico, there are several regions, where coastlines are composed of sediment muds (*i.e.*, cohesive terrigenous sediments), such as the inshore Southern coast line in the areas of Guanica Bay, Guayanilla Bay, from Ponce to Guayama; in the Western coast line, from South Rincon to inshore Mayagüez Bay; and in the Northern coastline in the Manati Bay. The midshore and offshore areas of the Southern and Western insular shelves are composed of reef and carbonate sands (*i.e.*, biogenic sediments) hardgrounds. Other Puerto Rico coastlines are mainly made of reef and carbonate sands hardgrounds (*op. cit.*).

Few studies have described the effects of episodic events in the Caribbean Sea on phytoplankton blooms, using hydrological and remote sensing data (Gilbes *et al.*, 2001). Therefore, in the case of our research we used hydrological and remote sensing data in order to investigate long-term trends in water quality in Puerto Rico.

2 METHODOLOGY

In the following section, background information about the three data types is presented. In addition, some facts about the study area are displayed as well as the procedures, objectives, and hypotheses.

2.1 Data Products

Two satellite data standard products were used to evaluate water quality parameters in this study. Near-surface phytoplankton chlorophyll *a* concentration ([Chla]), in milligram per cubic meter mg/m^3), was derived from the SeaWiFS algorithm (Maritorena and O'Reilly, 2000; O'Reilly *et al.*, 1998, 2000), which was later upgraded (Hu, Lee, and Franz, 2012). The second satellite data product was the diffuse vertical attenuation coefficient for downward irradiance at 490nm (Kd490), over the first optical attenuation layer, in per meter (m^{-1}). Data reprocessing was performed in 2012 for MODIS Aqua (Hu, Lee, and Franz, 2012).

The SeaWiFS sensor (1997-2010) was onboard of the SeaStar spacecraft. The spatial resolution of the data was 1.1km Merged Local Area Coverage (MLAC). The temporal resolution of the data was daily (Feldman and McClain, 2014).

The MODIS sensor (2002-Present) is onboard of the Aqua Earth Observing System ascending node (EOS PM-1) spacecraft. The MODIS sensor was developed by National Aeronautics and Space Administration (NASA), and launched on May 4, 2002 (Frazier and Maccherone, 2014). The spatial resolution of the data is at 1km Local Area Coverage (LAC). The temporal resolution was daily (Feldman and McClain, 2014). Both of these data products from these two sensors were retrieved from the OceanColor web site (*http://oceancolor.gsfc.nasa.gov/cgi/browse.pl?sen=am*) as Level 2 products (Feldman and McClain, 2014). Level 2 satellite products (only available at daily temporal resolution) were selected over Level 3 products (available at daily, monthly, and yearly temporal resolutions) because of higher and more appropriate spatial resolutions for the study of coastal waters. Level 3 spatial resolution of SeaWiFS data was 9km and of MODIS Aqua data 4km and 9km. Level 2 spatial resolution of SeaWiFS data was 1.1km and of MODIS Aqua 1km.

The river streamflow discharge, in cubic feet per second (ft^3/s) was retrieved from the USGS Water Information System web site (*http://waterdata.usgs.gov/pr/nwis/sw*) and (*http://wdr.water.usgs.gov/allsearch.php#sw*) as daily products.

2.2 Level 2 Chlorophyll a concentration satellite algorithms

The SeaWiFS [Chla] satellite algorithm (OC4S) was used as input (Table 1), the maximum band ratio (MBR) among the following remote sensing reflectances (Rrs), Rrs 443, 490, or 510 (as numerator), over Rrs 550 (as denominator) values, with a quadratic equation (a), and specific coefficients (Feldman and McClain, 2014).

By analogy, the MODIS Aqua [Chla] satellite algorithm (OC3M) was used as input (Table 2), the maximum band ratio (MBR) among the following remote sensing reflectances (Rrs), Rrs 443, 488 (as numerator), over Rrs 547 (as denominator) values, with a quadratic equation (b), and specific coefficients. The output for algorithms was near-surface phytoplankton chlorophyll *a* concentration [Chla], in mg/m^3 (Feldman and McClain, 2014).

The respective [Chla] algorithms were listed below, respectively:

OC4S: $C\alpha$: $10 \wedge (a_0 + a_1R_{4S} + a_2R^2_{4S} + a_3R^3_{4S} + a_4R^4_{4S})$ (a)

With $R_{4S} = \log_{10}$ (max Rrs 443, 490, 510 / Rrs 555)

a = [0.3272, -2.9940, 2.7218, -1.2259, -0.5683]

OC3M: $C\alpha$: $10 \wedge (a_0 + a_1R_{3M} + a_2R^2_{3M} + a_3R^3_{3M} + a_4R^4_{3M})$ (b)

With $R_{3M} = \log_{10}$ (max Rrs 443, 488 / Rrs 547)

a = [0.2424, -2.7423, 1.8017, 0.0015, -1.2280]

2.3 Level 2 Diffuse vertical attenuation coefficient satellite algorithms

The SeaWiFS Kd490 satellite algorithm (KD2S) was used as input (Table 1), the band ratio of the following remote sensing reflectances (Rrs), Rrs 490 (as numerator), over Rrs 555 (as denominator) values, with a quadratic equation (c), and specific coefficients (Feldman and McClain, 2014).

Table 1. *An overview of SeaWiFS bands and wavelengths (Feldman and McClain, 2014)*

Band	Wavelength (nm)
1	402-422
2	433-453
3	480-500
4	500-520
5	545-565
6	660-680
7	745-785
8	845-885

Table 2. *An overview of MODIS Aqua bands and wavelengths (Feldman and McClain, 2014)*

Band	Wavelength (nm)
8	405-420
9	438-448
10	483-493
11	526-536
12	546-556
13	662-672
14	673-683
15	743-753
16	862-877

By analogy, the MODIS Aqua Kd490 satellite algorithm (KD2M) was used as input (Table 2), the band ratio the following remote sensing reflectances (Rrs), Rrs 488 (as numerator), over Rrs 547 (as denominator) values, with a quadratic equation (d), and specific coefficients. The output for algorithms was diffuse vertical attenuation coefficient at 490nm, Kd490, in m^{-1} (Feldman and McClain, 2014).

The respective Kd490 algorithms were listed below, respectively:

KD2S: Kd490: $10 \wedge (a_0 + a_1 Kd_{2S} + a_2 Kd^2_{2S} + a_3 Kd^3_{2S} + a_4 Kd^4_{2S})$ (c)

With $Kd_{2S} = \log_{10}$ (Rrs 490 / Rrs 555)

a = [-0.8515, -1.8263, 1.8714, -2.4414, -1.0690]

KD2M: Kd490: $10 \wedge (a_0 + a_1 Kd_{2M} + a_2 Kd^2_{2M} + a_3 Kd^3_{2M} + a_4 Kd^4_{2M})$ (d)

With $Kd_{2M} = \log_{10}$ (Rrs 488 / Rrs 547)

a = [-0.8813, -2.0584, 2.5878, -3.4885, -1.5061]

2.4 River streamflow discharge

Instantaneous / mean daily discharges were used from the United States Geological Survey (USGS) National Water Information System (NWIS) (*e.g.*, Díaz *et al.*, 1998). The output was river streamflow discharge, 0.028317 cubic meters per second [m^3/s; cubic feet per second (ft^3/s)]

2.5 Study area

The study area measured 159,100 km^2, which covered from 16^oN to 20^oN latitudes and from -68^oW to -64^oW longitudes, from Isla Mona to the U.S. Virgin Island. Surface water data of 12 river study sites in Puerto Rico, from 1998 to 2013, were used to analyze the river streamflow discharge (Figure 1). These rivers were grouped into four regions (*i.e.*, West, North, East, and South of Puerto Rico).

The Western river stations were Rio Culebrinas, Rio Grande de Añasco, and Rio Guanajibo; the Northern river stations were Rio Grande de Arecibo, Rio Grande de Manati, Rio de La Plata, and Rio Grande de Loiza; the Eastern river stations were Rio Fajardo and Rio Humacao; the Southern river stations were Rio Cerrillos, Rio Jacaguas, and Rio Guayanilla. Their watershed basins were illustrated (Figure 1).

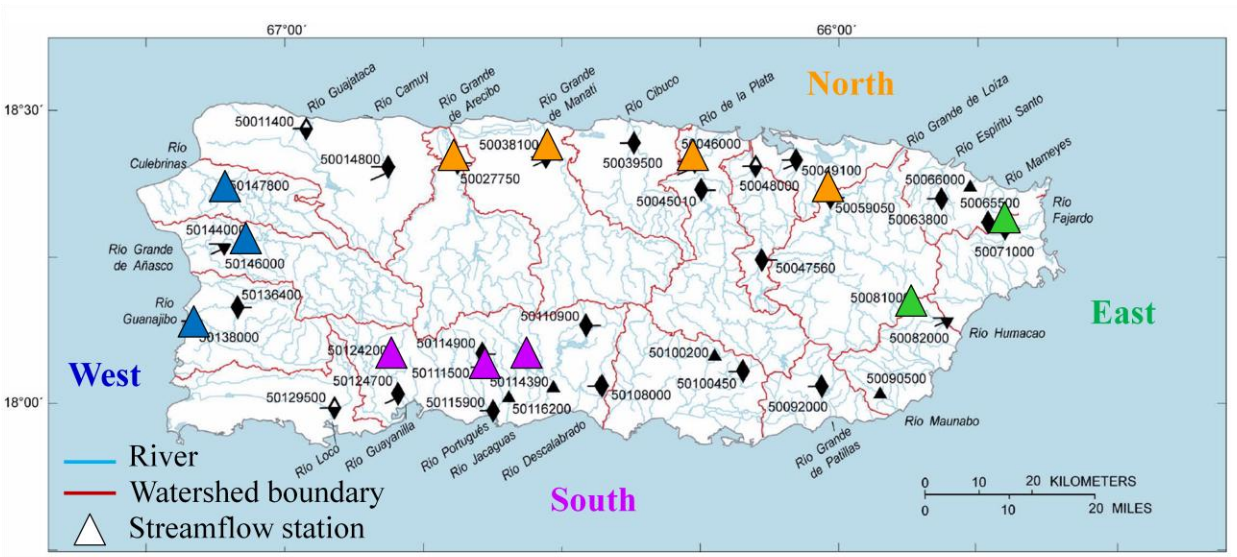

Figure 1. Locations of the river streamflow stations in Puerto Rico (Díaz *et al*., 1998)

2.6 River discharge procedure

The daily river streamflow discharge was composed of around 70,500 data input, which comprised a period of 16 years and of 12 river surface-water stations (Figures 2 and 4). Microsoft Excel 2007 was used to input the USGS daily river streamflow discharge data for each of the river surface-water stations, which were collected and averaged by region. Then, each region was averaged to produce annual and seasonal time series (*i.e.*, rainy and dry seasons) from 1998-2013.

2.7 Pixel selection procedure

The selection of the river sites' pixel locations was made by first collecting the latitudes and longitudes (lat/lon) of the river mouth of each respective site using Google Earth. To increase the chance of selecting a pure water pixel instead of a mixed water/land pixel (and minimize the effect of shallow water bottom reflectance, which could be greater closer to land), along the line tangent to the shelf edge, pixels at 2km away from the river mouth were used up to 16km away. SeaWiFS data were used from 1998 to 2009 and MODIS Aqua data were used from 2010 to 2013, for a total of 16-year time frame.

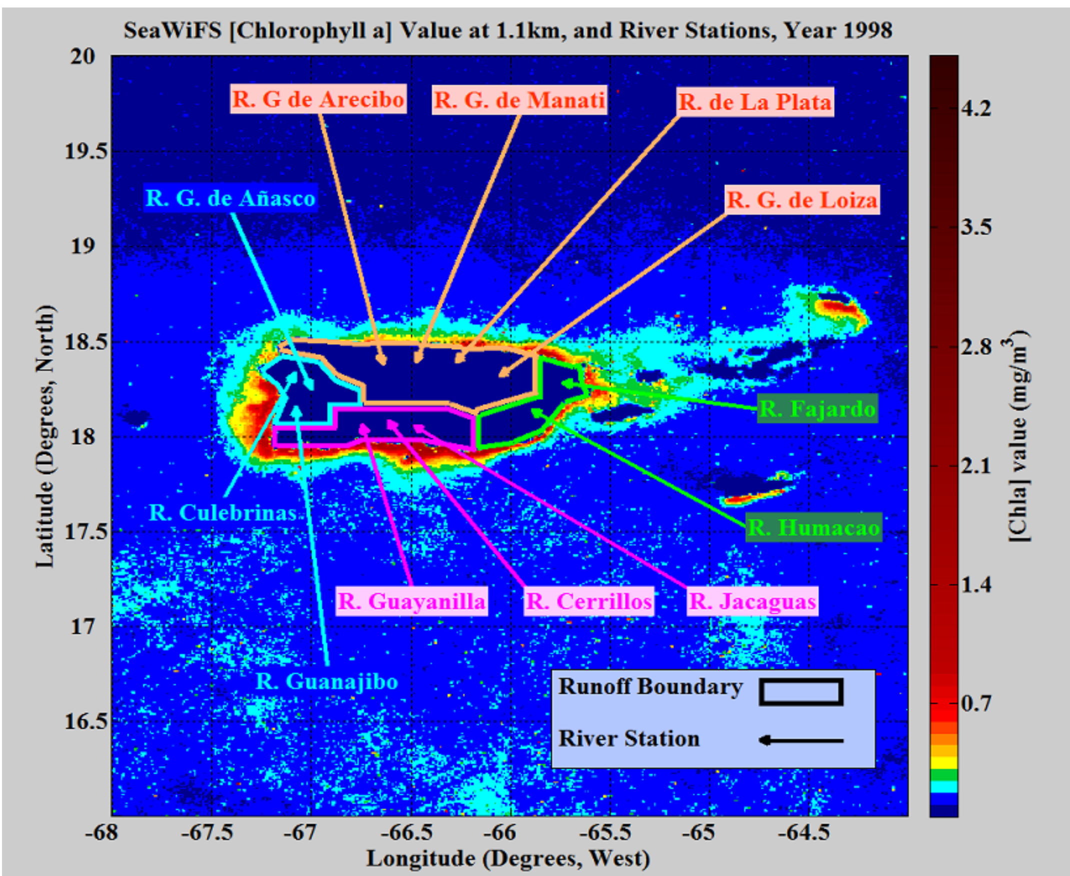

Figure 2. SeaWiFS [Chlorophyll *a*] image at 1.1km spatial resolution for 1998. The image indicated the location of surface water stations. The source of the river stations and watershed boundaries were from Díaz, *et al.* (1998)

2.8 Preprocessing software procedure

The SeaWiFS Data Analysis System (SeaDAS) software package was used to perform data visualization (Baith *et al.*, 2001). Around 11000 SeaWiFS and 4000 MODIS Aqua uncompressed data files were screened and pre-processed. SeaDAS v6.4 was used for accurately reprojecting and ortho-rectifiying all the daily [Chla] and Kd490 input (Hierarchical Data Format, HDF) data files. Only data files with minimal or no pixel distortions, and cloud-free were selected for the study.

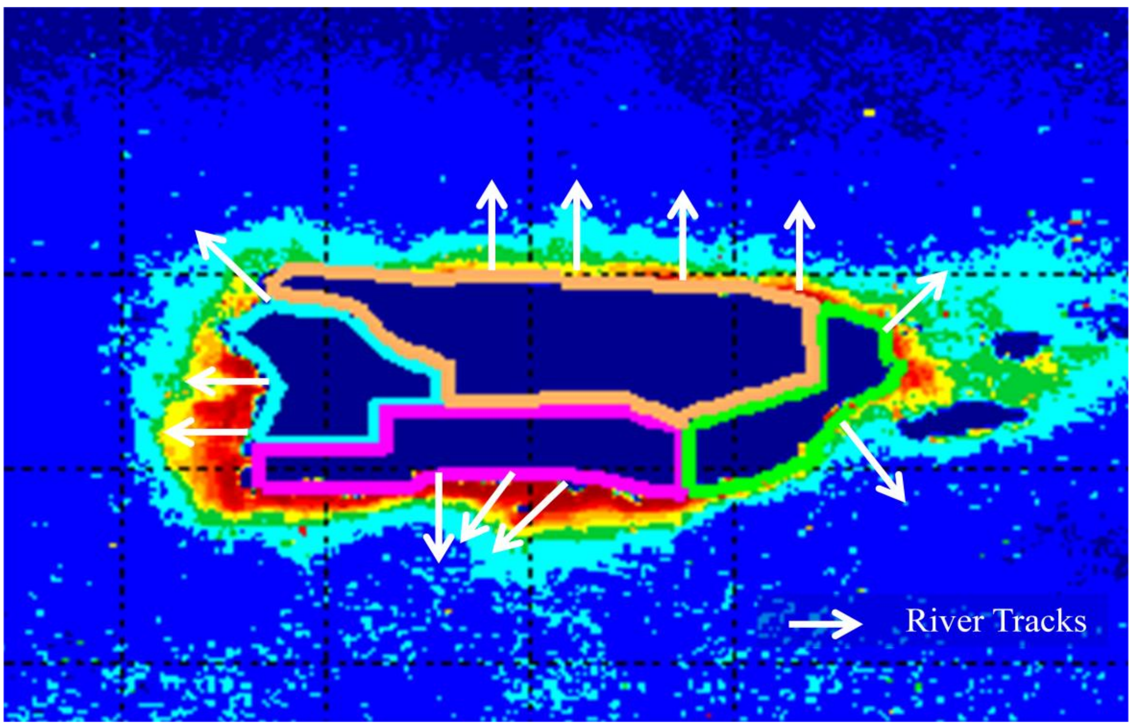

Figure 3. SeaWiFS [Chlorophyll *a*] close-up image at 1.1km spatial resolution for 1998. The image indicated the river tracks of surface water stations from 2km to 16km from the river mouth. The source of the watershed boundaries were from Díaz, *et al.* (1998)

2.9 Processing software procedure

All data processing, imaging, and analyses were performed by writing and running scripts using the software package MATrix LABoratory (MATLAB version 7.12.0, The MathWorks Inc., Natick, MA, 2011). The daily data files selected were checked for suitability as input files, and transformed into monthly and annual averages, and then into seasonal averages. The input river track sites' [Chla] and Kd490 values (*i.e.*, 2km to 16km from the river mouth) were extracted (Figure 3) from each annual and seasonal data files and grouped into the four regions. Finally, annual and seasonal time series (*i.e.*, rainy and dry seasons) from 1998-2013 were used to create the regional trend graphs and maps. The Pearson's correlation coefficients were calculated and graphed and displayed in maps for Kd490 and [Chla], Kd490 and river discharge, and [Chla] and river discharge values.

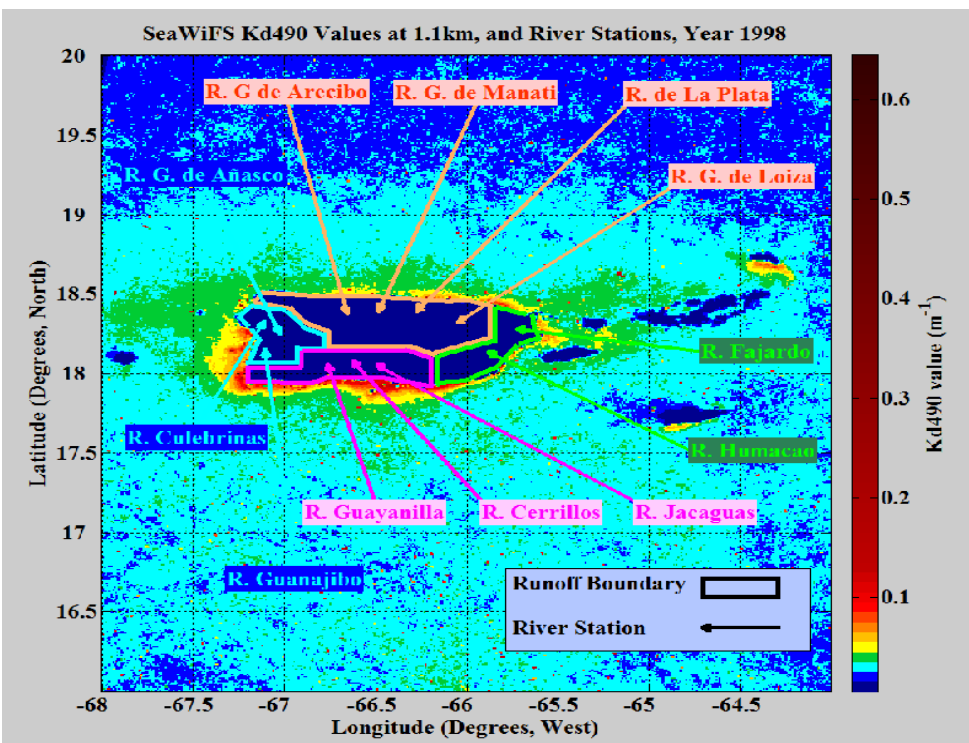

Figure 4. SeaWiFS Kd490 image at 1.1km spatial resolution for 1998

2.10 Objectives

The present study had two main objectives; to investigate long-term (16-year) trends in water quality parameters (*i.e.*, [Chla] and Kd490), and river streamflow discharge, in relation to regional and temporal resolutions, in coastal waters of Puerto Rico, and to examine how these parameters were temporally and regionally correlated.

The following hypotheses were tested:

1. There was a decreasing trend in Kd490 and [Chla] in the coastal waters of Puerto Rico from 1998 to 2013.
2. Seasonal and regional patterns of [Chla] in coastal waters were correlated with Kd490.
3. Seasonal and regional patterns in Kd490 in coastal regions were directly proportional to the river discharge.
4. [Chla] concentration in coastal areas was directly proportional to seasonal and regional patterns of river discharge.

3 RESULTS

The [Chla] and Kd490 data at 2km distance from the river mouth were selected since it was most representative of the river mouth and not too close to land/water pixel mix or shallow water bottom reflectance. For the period between 1998 to 2013, the [Chla], Kd490, and river discharge regional trends were evaluated annually and seasonally. The Pearson correlation coefficients (r) between Kd490 and [Chla], Kd490 and river discharge, and [Chla] and river discharge, for each of the river regions were assessed annually, and during the rainy and dry seasons. In this study, a range of values were used to describe the correlation results as follows: 0 – No, +/- 0.01-0.19 –

Slight, +/- 0.20-0.29 – Weak, +/- 0.30-0.39 – Moderate, +/- 0.40-0.69 – Strong, and greater +/- 0.70 – Very strong.

3.1 [Chla] and Kd490

In general, the annual [Chla] and Kd490 decreased with time from 2km to 16km away from the river mouth, even thought, there were periods of increasing patterns (*e.g.*, major and intermediate peaks). However, this decrease was moderately observable from 2 to 6km away from the river mouth. From 7km to 16km away from the river mouth, the [Chla] and Kd490 were weakly to slightly decreasing.

During the rainy season, the [Chla] and Kd490 decreased in a similar trend, but at different intensity than were the annual data. Also, during the dry season, the [Chla] and Kd490 diminished in an analogous distance patterns.

3.1.1 [Chla]

The annual scatter plots of [Chla] for 2km away from the river mouth, for each river of each of the four regions were illustrated (Figure 5a-5d).

Annually, at 2km from the river mouth, in each region, there were major peaks and intermediate peaks of [Chla] during 1998 to 2013. However, these peaks did not occur on same years for each river, within each region. The main peaks of [Chla] for the Western rivers were in 1999, 2002, and 2005. After 2005, each river had its own pattern. Rio Grande de Añasco seemed to be the major river driving the relationship among the Western rivers. The main peaks of [Chla] for the Northern rivers were in 1998, 2003, and 2011. The main peaks of [Chla] for the Eastern rivers appeared to be inversely related between the two rivers. The main peaks of [Chla] for the Southern rivers were in 1998, 2002, and 2010. Rio Guayanilla looked to be the major river driving the relationship in the Southern rivers. Annually, the main peaks of [Chla] that were occurring in all four regions occurred in 1998, and between 2010 and 2011. Hence, there was variability in annual [Chla] among regions and within each region. Similar patterns were found during the rainy and dry seasons.

As a result, the [Chla] mean for each region was taken to better perceive the major peaks, and to evaluate the trends during 1998-2013. The annual scatter plots of [Chla] for 2km away from the river mouth, for each of the four river regions were illustrated, including the equation of the trend line, and the trend percent change value (Figure 6a-6d). Annually, at 2km from the river mouth, for each region, there were major peaks and intermediate peaks of [Chla] during 1998 to 2013. The main peaks of [Chla] for the Western rivers were in 1999, 2002, and 2010. The intermediate peaks were in 2006 and 2008. The main peaks of [Chla] for the Northern rivers were in 1998, 2003, and 2011. The main peaks of [Chla] for the Eastern rivers were in 2003, 2005, and 2007. The main peaks of [Chla] for the Southern rivers were in 1998, 2002, and 2010. Hence, there was variability in annual [Chla] among regions.

By comparison, during the rainy season, the main peaks of [Chla] that were occurring in all four regions occurred in 1998, and between 2010 and 2011. Hence, there was variability in rainy season [Chla] among regions and within each region.

By contrast, during the dry season, the main peaks of [Chla] that were occurring in all four regions occurred in 1999. Hence, there was variability in the dry season [Chla] among regions, but less variability within each region, compared to the annual and rainy seasons.

The results showed that trends in [Chla] percent changed, at 2km from the river mouth varied from 1998 to 2013. In the annual trends (Figures 6 and 11), only the Western rivers had a weak

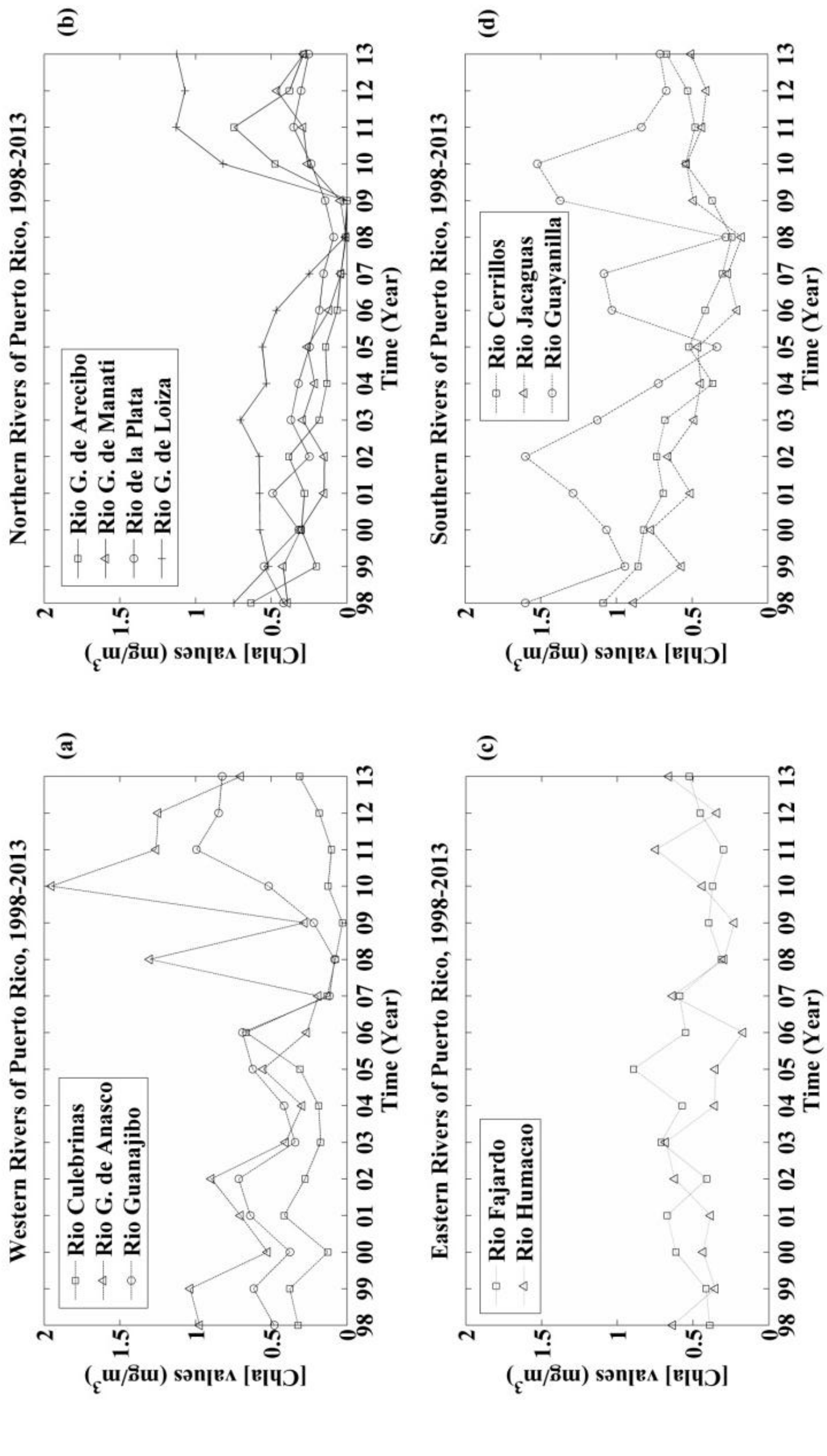

Figure 5. Chlorophyll *a* concentration annual mean values, of (a) Western Rivers, (b) Northern Rivers, (c) Eastern Rivers, and (d) Southern Rivers, 2km away from the river mouth, Puerto Rico, 1998-2013

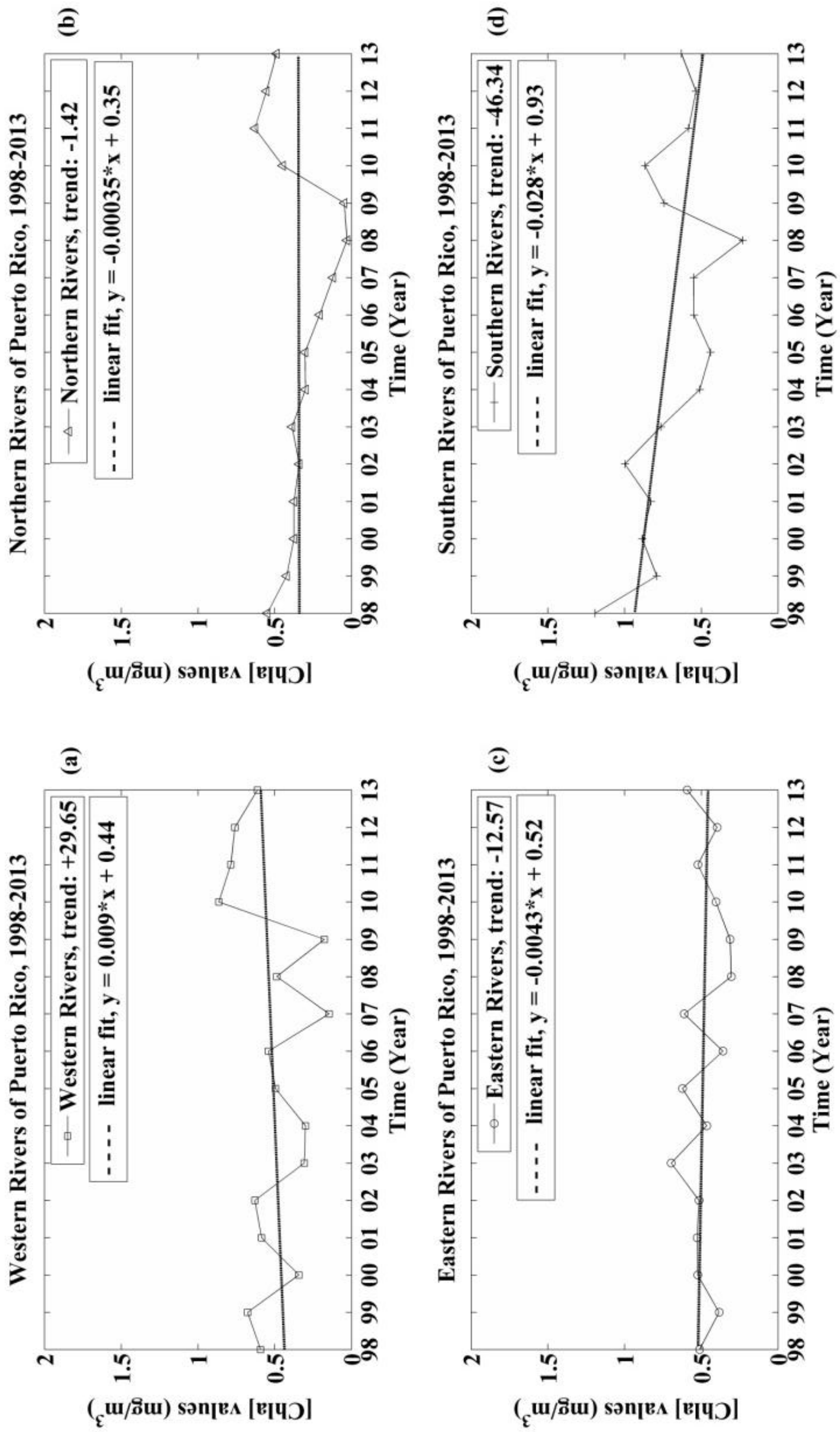

Figure 6. Chlorophyll a concentration annual regional mean and trend percent values, of (a) Western Rivers, (b) Northern Rivers, (c) Eastern Rivers, and (d) Southern Rivers 2km away from the river mouth, Puerto Rico, 1998-2013

increasing trend (*i.e.*, 29.65%), whereas, the other three river regions had a gradient of slight to strong decreasing trend (*i.e.*, Northern -1.42%, Eastern -12.57%, and Southern -46.34%).

During the rainy season (Figure 12), the Western region had a very strong increasing trend, which was around 2.84 times greater than the annual trend (*i.e.*, 83.97%). The Northern region slight decreasing seasonal trend was around 10 times greater than annually (*i.e.*, -14.17%).

The Eastern and Southern regions, respectively, had a slight and strong decreasing trends that did not change much (*i.e.*, -13.69% and -44.49%).

During the dry season (Figure 13), the Western rivers had a slight decreasing trend (*i.e.*, -4.83%). The Eastern and Southern regions had a slight to strong decreasing trends and were a bit higher than during the rainy season (*i.e.*, -18.06% and -52.08%). To the contrary, the Northern regions had a slight increasing trend (*i.e.*, 17.09%).

In summary, the maximal range for the annual, rainy and dry seasons [Chla] values for the four regions in decreasing order was Southern, Western, Eastern, and Northern. Also, there was temporal and spatial variation in the [Chla] annual and seasonal trends.

3.1.2 Kd490

The annual scatter plots of Kd490 for 2km away from the river mouth, for each river of each of the four regions were illustrated (Figure 7a-7d).

Annually, at 2km from the river mouth, in each region, there were major peaks and intermediate peaks of Kd490 during 1998 to 2013. However, these peaks did not occur on same years for each river, within each region. The main peaks of Kd490 for the Western rivers were in 1999. After 2005, each river had its own pattern. Rio Grande de Añasco seemed to be the major river driving the relationship in the Western rivers. The main peaks of Kd490 for the Northern rivers were not very discernible. The main peaks of Kd490 for the Eastern rivers seemed to be inversely related between the two rivers. The main peaks of Kd490 for the Southern rivers were in 1998, 2002, and 2010. Rio Guayanilla looked to be the major river driving the relationship in the Southern rivers. Annually, the main peaks of Kd490 that were occurring in all four regions occurred in 1998 and 1999. Hence, there was variability in annual Kd490 among regions and within each region. Similar patterns were observed during the rainy and dry seasons.

As a result, the Kd490 mean for each region was used to better perceive the major peaks, and to evaluate the trends during 1998-2013. The annual scatter plots of Kd490 at 2km away from the river mouth, for each of the four river regions were shown, including the equation of the trend line, and the seasonal trend percent change value (Figure 8a-8d). Annually, at 2km from the river mouth, for each region, there were major peaks and intermediate peaks of Kd490 during 1998 to 2013. The main peaks of Kd490 for the Western rivers were in 1999, 2002, and 2010. The intermediate peaks were in 2006 and 2008. The main peaks of Kd490 for the Northern rivers were in 1998, 2000, and 2011. The main peaks of Kd490 for the Eastern rivers were in 2002, 2006, and 2011. The main peaks of Kd490 for the Southern rivers were in 1998, 2002, and 2010. Hence, there was variability in the annual Kd490 among regions.

By contrast, during the rainy and dry seasons, there were no discernible main peaks of Kd490 that were occurring in all four regions. However, there was variability in the rainy and dry seasons Kd490 among regions.

The trends in Kd490 percent change, at 2km from the river mouth, varied from 1998 to 2013. In the annual trends (Figures 8 and 11), only the Western rivers had a slight increasing trend (*i.e.*, 5.90%), whereas, the other three river regions had a gradient of slight to strong decreasing trend (*i.e.*, Northern -12.06%, Eastern -12.98%, and Southern -56.87%).

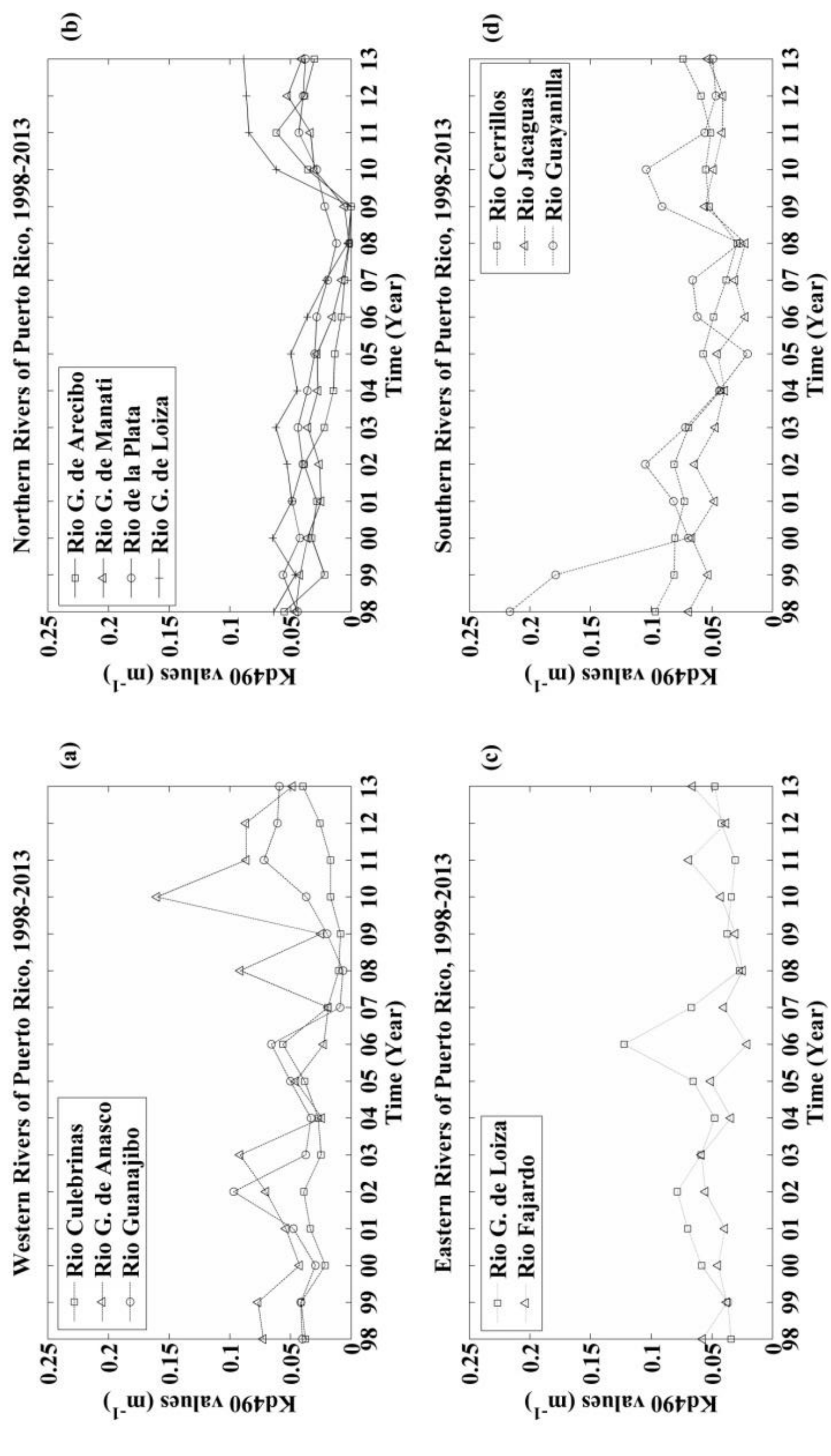

Figure 7. Kd490 annual mean values, of (a) Western Rivers, (b) Northern Rivers, (c) Eastern Rivers, and (d) Southern Rivers, 2km away from the river mouth, Puerto Rico, 1998-2013

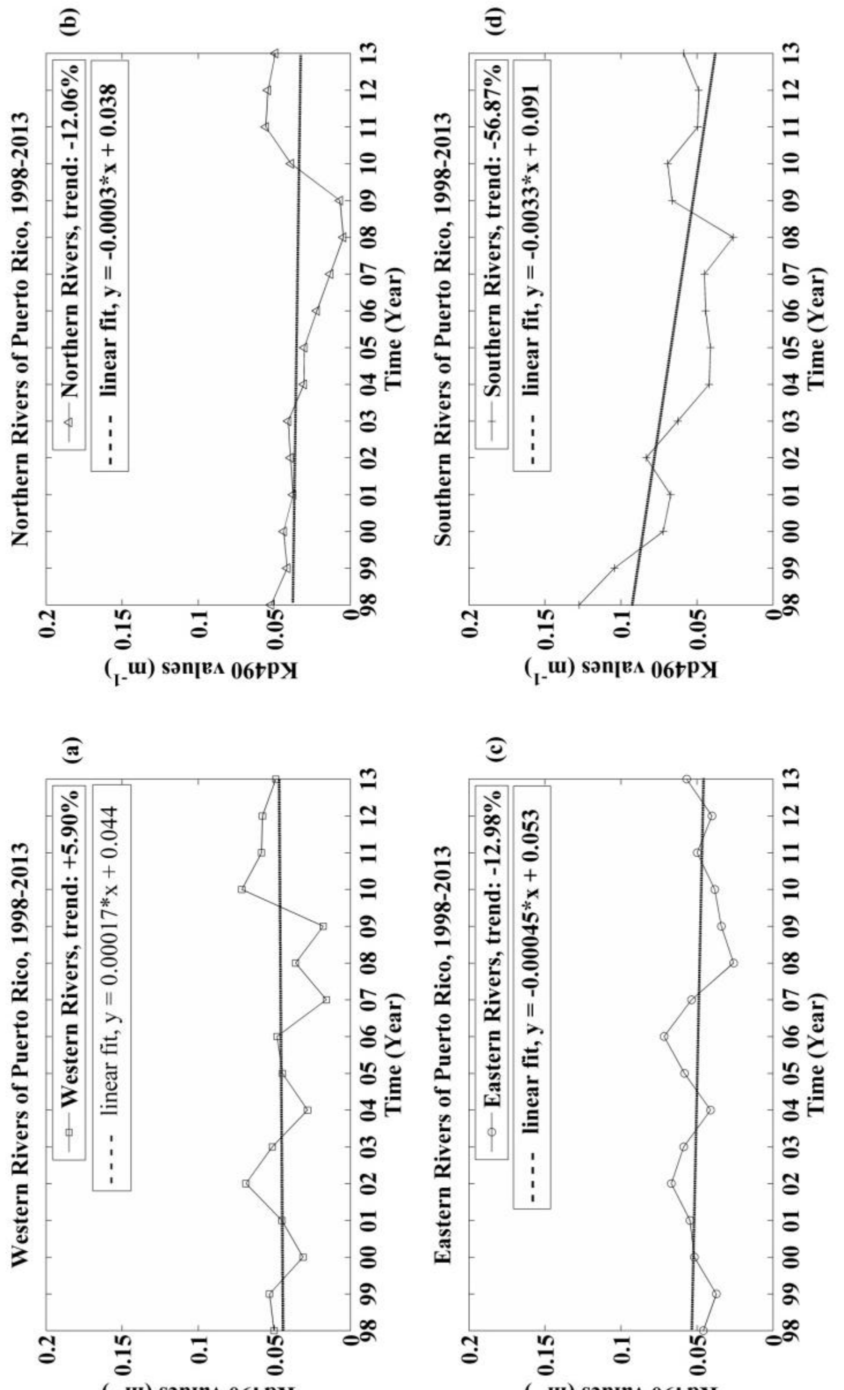

Figure 8. Kd490 annual regional mean values, of (a) Western Rivers, (b) Northern Rivers, (c) Eastern Rivers, and (d) Southern Rivers, 2km away from the river mouth, Puerto Rico, 1998-2013

During the rainy season (Figure 12), the Western region moderate increasing trend was around 5.91 times greater than the annual trend (*i.e.*, 34.86%). The Northern and Eastern regions weak decreasing trends were, respectively, around 2.16 and 2.29 times greater than the annual trend (*i.e.*, -26.08% and -29.72%). The Southern region very strong decreasing trend increased, but did not change much (*i.e.*, -64.34%).

During the dry season (Figure 13), the Western rivers had a slight decreasing trend (*i.e.*, -17.12%). The Southern region had a strong decreasing trends and much lower than during the rainy season (*i.e.*, -46.73%). To the contrary, the Northern and Eastern rivers had slight increasing trends (*i.e.*, 3.13% and 0.20%).

Similarly to [Chla], the maximal range for the annual, rainy, and dry season Kd490 values for the four regions in decreasing order was Southern, Western, Eastern, and Northern. Also, there was temporal and spatial variation in the Kd490 annual and seasonal trends.

3.1.3 River Discharge

The annual scatter plots of river discharge in relation to the river mouth, for each river of each of the four regions were illustrated (Figure 9a-9d).

Annually, for the river mouth, in each region, there were major peaks and intermediate peaks of river discharge during 1998 to 2013. However, these peaks did not always occur on same years for each river, within each region. The main peaks of river discharge for the Western rivers were in 1998, 2005, and 2010. The main peaks of river discharge for the Northern rivers were in 1998, 2004/2005, 2010/2011. The main peaks of river discharge for the Eastern rivers were in 1998, 2005, and 2011. The main peaks of river discharge for the Southern rivers were in 1998, 2005 and 2011. Annually, the main peaks of river discharges that were occurring in all

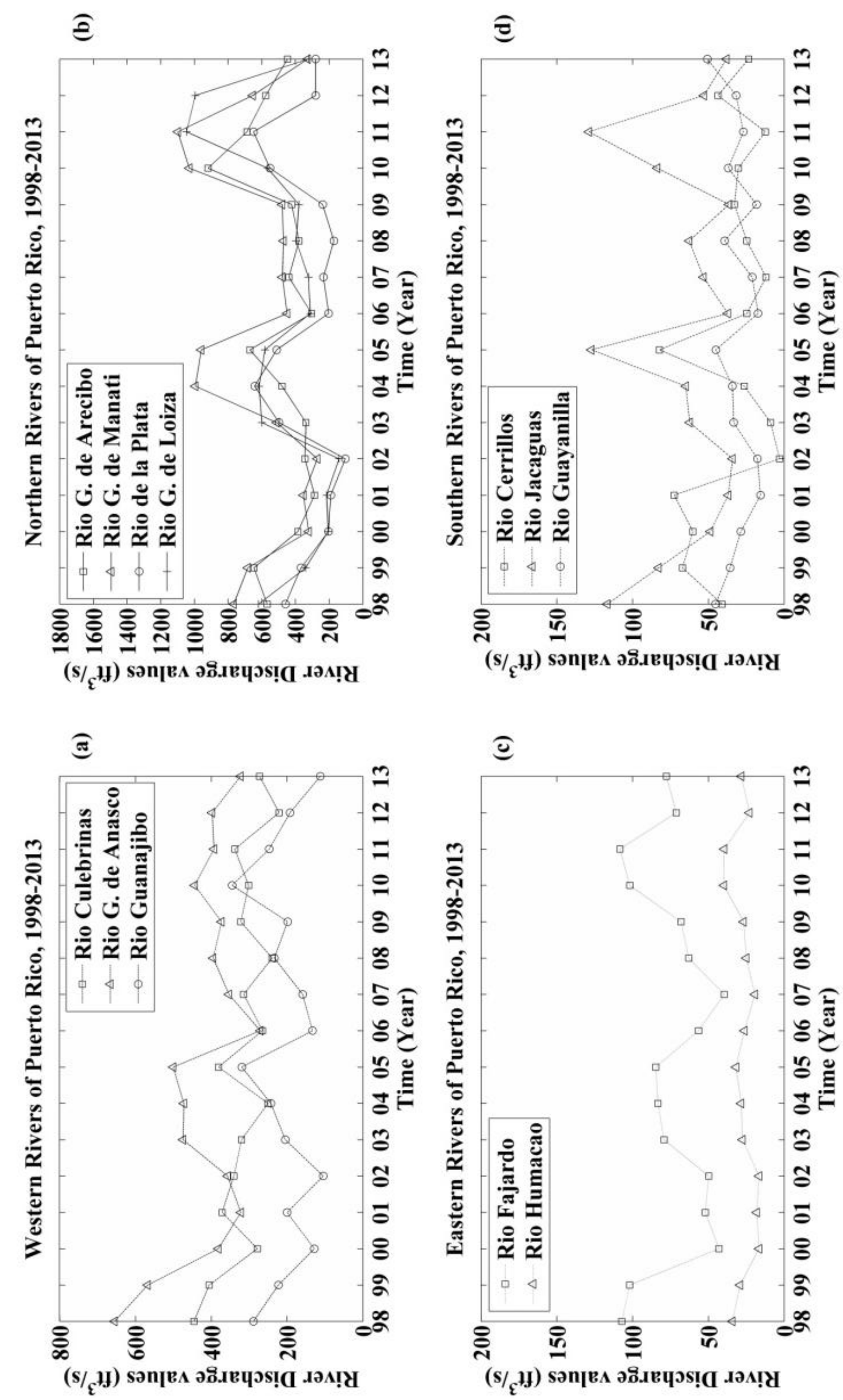

Figure 9. River discharge annual mean values, of (a) Western Rivers, (b) Northern Rivers, (c) Eastern Rivers, and (d) Southern Rivers, for the river mouth, Puerto Rico, 1998-2013

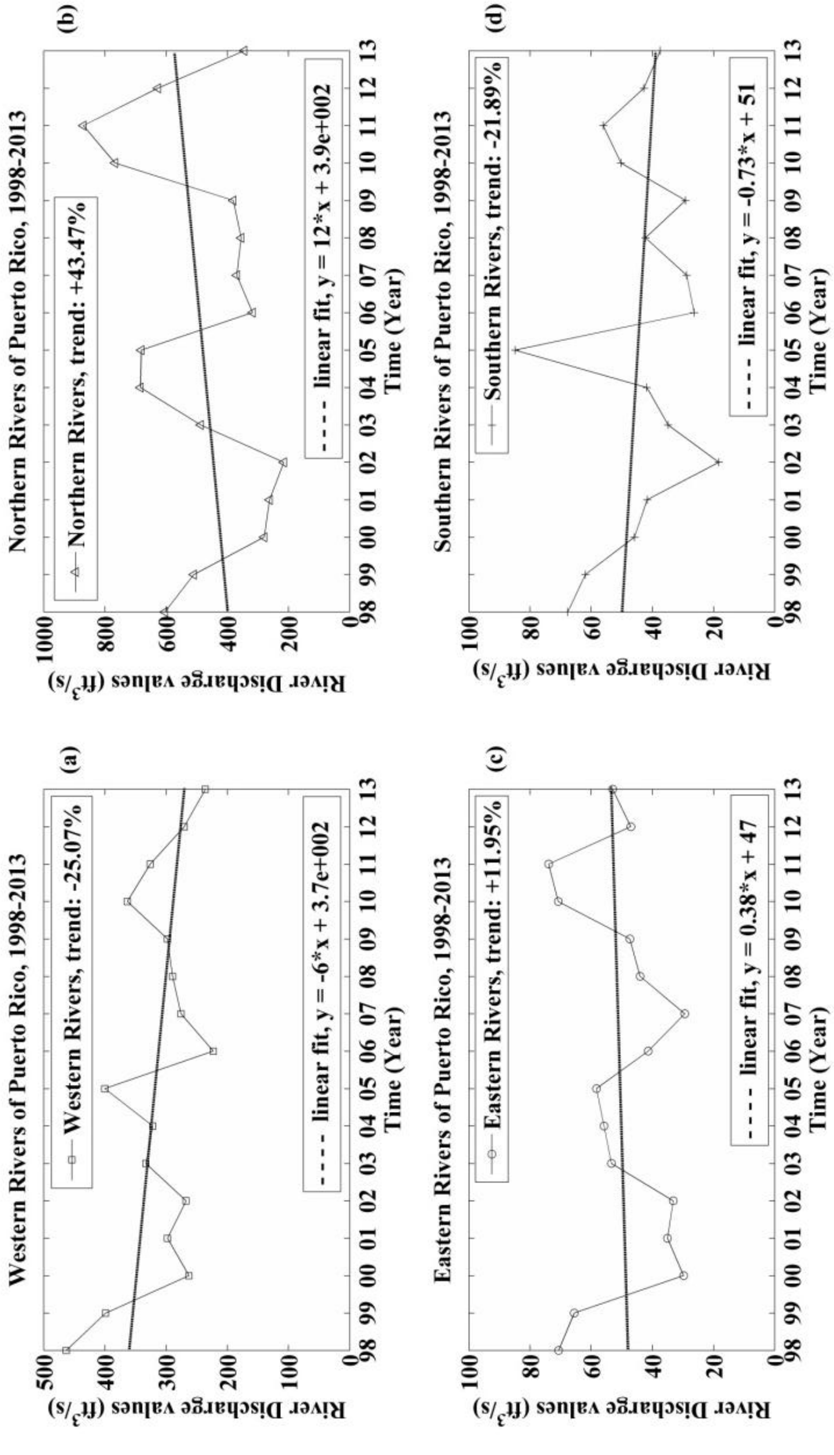

Figure 10. River discharge, annual regional mean values, of (a) Western Rivers, (b) Northern Rivers, (c) Eastern Rivers, and (d) Southern Rivers, for the river mouth, Puerto Rico, 1998-2013

four regions occurred in 1998, and between 2010 and 2011. Hence, there was variability in annual river discharge among regions and within each region.

As a result, the mean river discharge for each region was taken to better perceive the major peaks, and to evaluate the trends during 1998-2013. The annual scatter plots of river discharge for the river mouth, for each of the four river regions were illustrated, including the equation of the trend line, and the annual trend percent change value (Figure 10a-10d). Annually, for the river mouth, for each region, there were major peaks and intermediate peaks of river discharge during 1998 to 2013. The main peaks of river discharge for the Western rivers were in 1998, 2005, and 2010. The main peaks of river discharge for the Northern rivers were in 1998, 2004, and 2011. The main peaks of river discharge for the Eastern rivers were in 1998, 2005, and 2011. The main peaks of river discharge for the Southern rivers were in 1998, 2005, and 2011. Hence, there was variability in the annual river discharge among regions. The order of intensity of the three river discharge major peaks was not the same for each region. The Northern region had stronger river discharge than the Western region. For the Western region, the decreasing order was 1998, 2005, and 2011. For the Northern region, the decreasing order was 2011, 2005, and 1998, which was the inverse of the Western region pattern. The Southern region had stronger river discharge than the Eastern region. For the Eastern region, the decreasing order was 2011, 1998, and 2005. For the Southern region, the decreasing order was 2005, 1998, and 2011, which was the inverse of the Eastern region pattern.

By contrast, during the rainy and dry seasons, there were no discernible main peaks of river discharge that were occurring in all four regions. However, there was variability in the rainy and dry seasons river discharge among regions.

The trends in river discharge percent change, at the river mouth, from 1998 to 2013 varied. In the annual trends (Figure 10a-10d and 11), the Western and Southern rivers had a weak decreasing trend (*i.e.*, -25.07% and -21.89%, respectively) whereas, the other two river regions had a gradient of slight to moderate increasing trends (*i.e.*, Eastern 11.95% and Northern 43.47%).

During the rainy season (Figure 12), the Western and Southern regions showed moderate decreasing trends that were greater but did not change much than the annual trend (*i.e.*, -34.14% and -32.84%, respectively). The Northern region weak increasing trend was lower but did not change much than the annual trend (*i.e.*, 35.55%). The Eastern region slight increasing trend was slightly greater but did not change much than the annual trend (*i.e.*, 12.88%).

During the dry season (Figure 13), all the river regions showed increasing trends. The Western rivers had a slight increasing trend (*i.e.*, 9.30%). The Southern region had a weak increasing trend (*i.e.*, 25.81%). The Eastern rivers had a slight increasing trend (*i.e.*, 10.77%). The Northern rivers had a very strong increasing trend, 2.15 times as much as during the rainy season (*i.e.*, 76.31%).

In summary, the maximal range for the annual and rainy season river discharge values for the four regions in decreasing order was Northern, Western, Southern, and Eastern. The maximal range for the dry season river discharge values for the four regions in decreasing order was Northern, Western, Eastern, and Southern. There was variability in the regional annual, rainy, and dry river discharge among regions. Also, there was temporal and spatial variation in the river discharge annual and seasonal trends.

For the Western rivers, there were increasing annual trends in [Chla] and Kd490 (Figure 11), but a decreasing trend in river discharge. On the other hand, for the Northern and Eastern rivers, there were decreasing trends in [Chla] and Kd490 but an increasing trend in the river discharge. For the Southern rivers, there were decreasing trends in [Chla], Kd490, and river discharge.

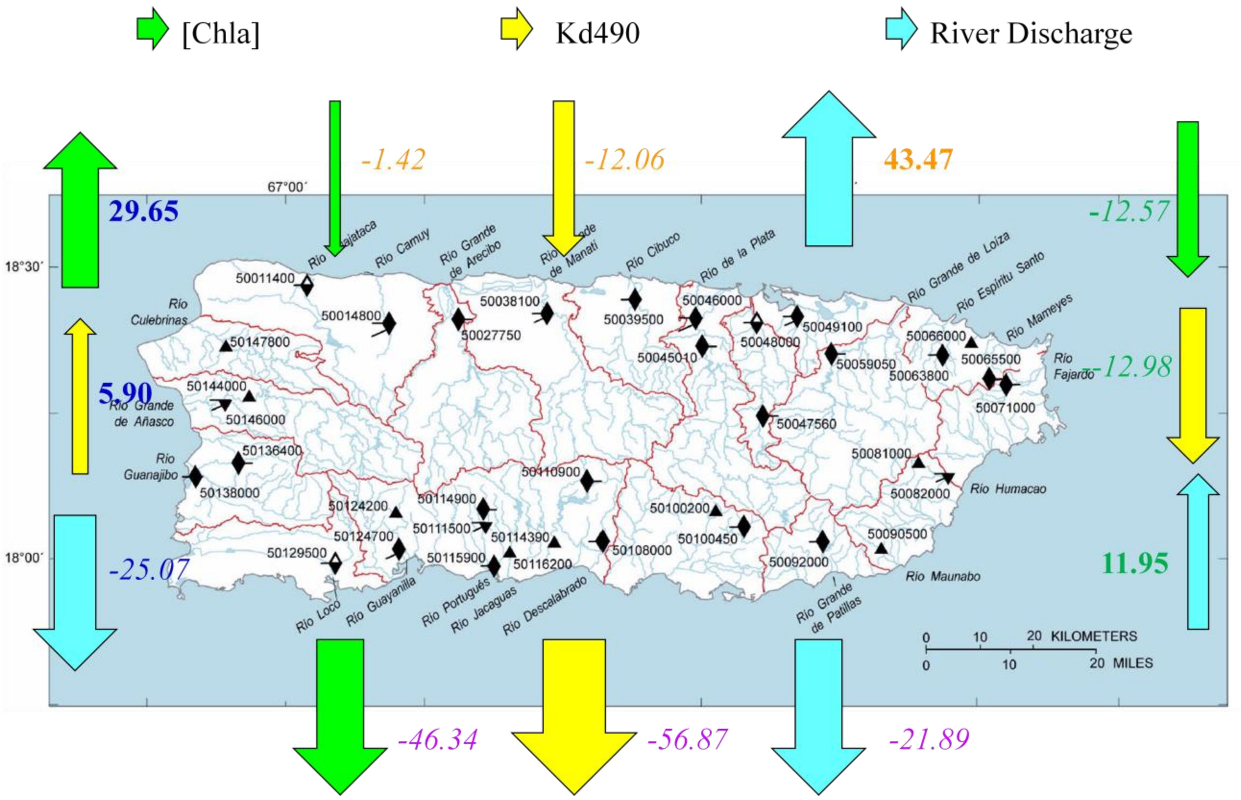

Figure 11. Annual percent trends of [Chla], Kd490, and river discharge, Puerto Rico, 1998-2013

During the rainy season (Figure 12), the trends were similar to the annual data, however, more or less intense depending on the region, especially for the Western and Northern rivers [Chla] and Kd490, but for the Northern river discharge and Southern river [Chla].

During the dry season the Western rivers had decreasing trend in [Chla] and Kd490, and an increasing trend in the river discharge (Figure 13). For the Northern rivers, there were increasing trends in [Chla], Kd490, and river discharge. For the Eastern rivers, there were a decreasing trend for [Chla], and increasing trends for Kd490 and river discharge. For the Southern rivers, [Chla] and Kd490 were in decreasing trends while the river discharge was an increasing trend.

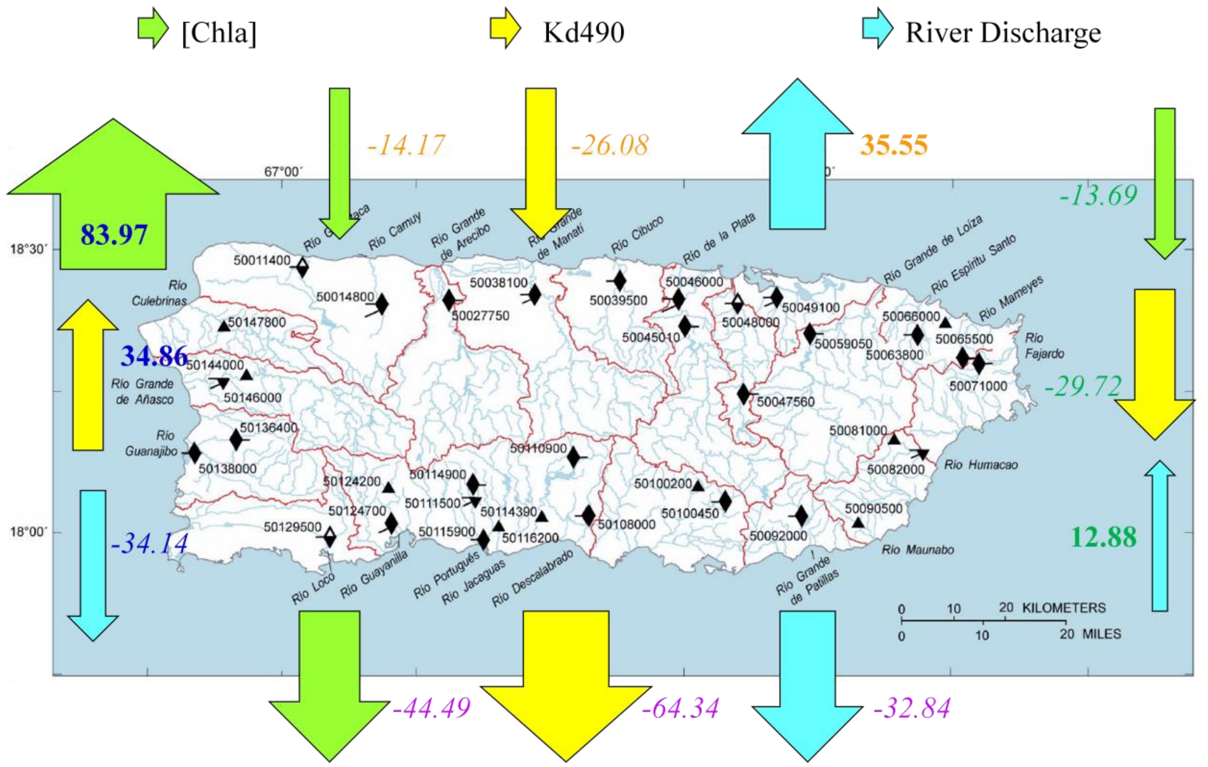

Figure 12. Rainy season percent trends of [Chla], Kd490, and river discharge, Puerto Rico, 1998-2013

3.2 Images of [Chla] and Kd490

The annual images of [Chla] and Kd490 for 1998, 2005, and 2011 were illustrated (Figures 14, 15, 16). From the annual river discharge results and graphs, the years with the major river discharge peaks (*i.e.*, 1998, 2005, and 2011) were selected to evaluate their relationships with [Chla] and Kd490.

In 1998 (Figure 14a-14b), the [Chla] and Kd490 in the coastal waters of Puerto Rico were the highest, followed by 2011 (Figure 16a-16b), and the least values in 2005 (Figure 15a-15b).

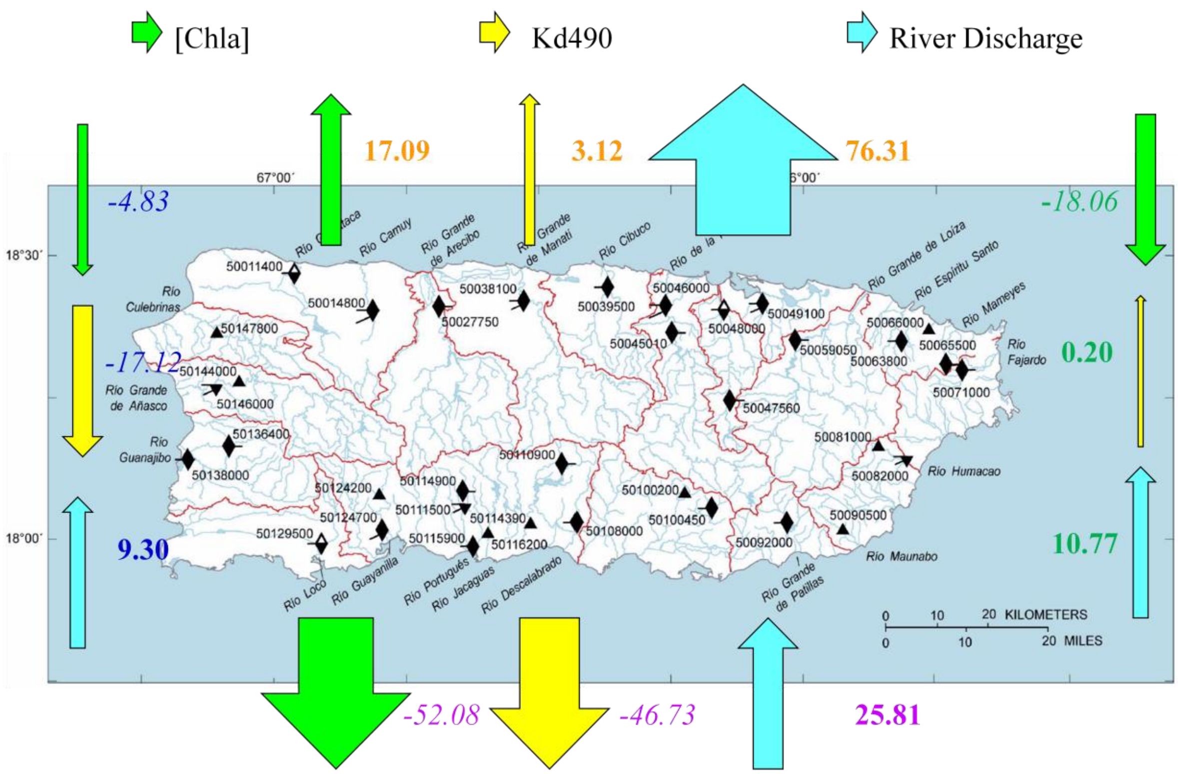

Figure 13. Dry season percent trends of [Chla], Kd490, and river discharge, Puerto Rico, 1998-2013

The lowest levels were located in the North, low levels in the East, high levels in the West, and the highest levels in the South.

Three daily data, which exhibited episodic events during 1998, were illustrated to show differences between the dry season (Figure 17a-17b) and the rainy season (Figure 18a-18b) and (Figure 19a-19b) events.

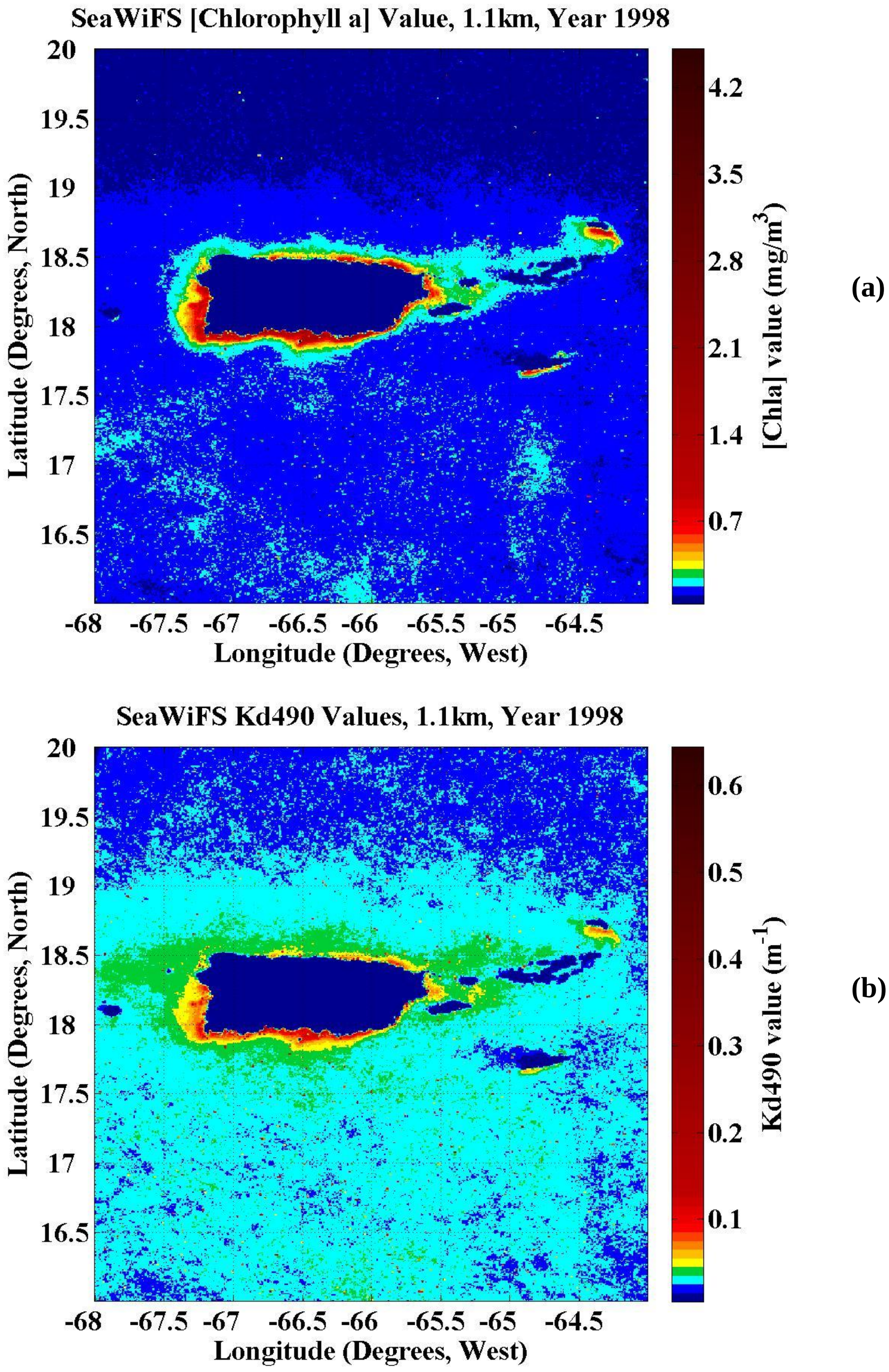

Figure 14. Study area image of SeaWiFS [Chlorophyll a] value (a) and Kd490 (b) for 1998

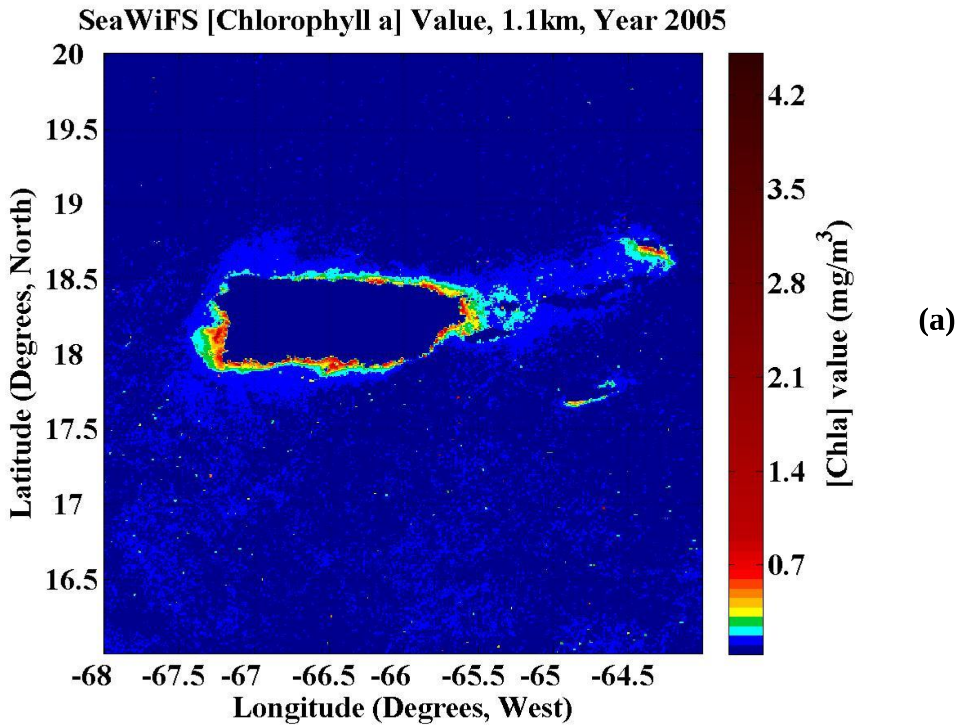

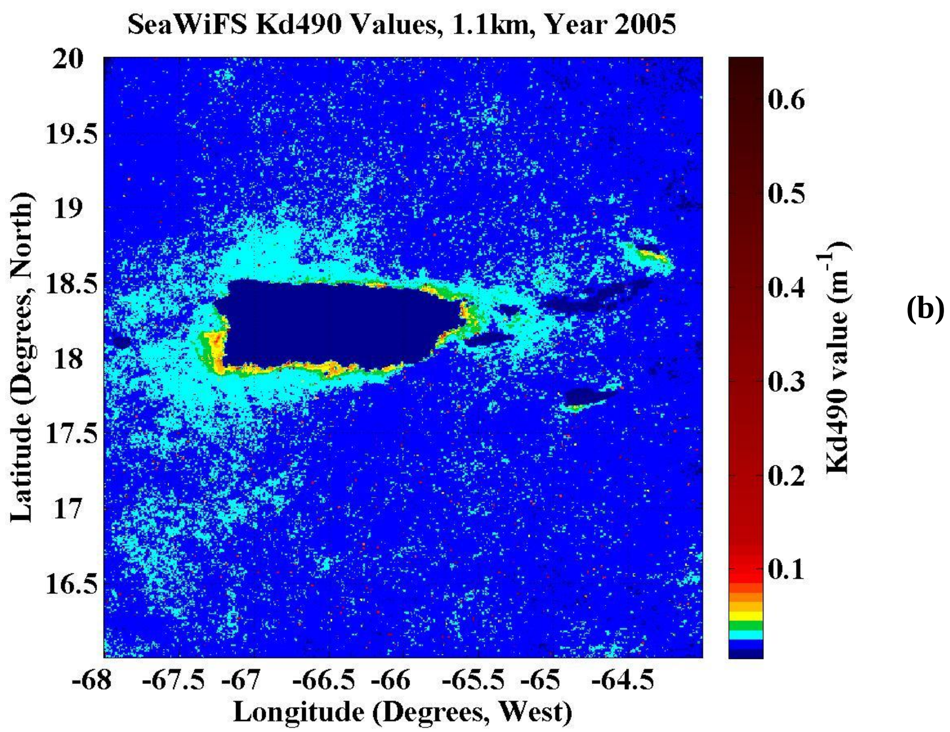

Figure 15. Study area image of SeaWiFS [Chlorophyll a] value (a) and Kd490 (b) for 2005

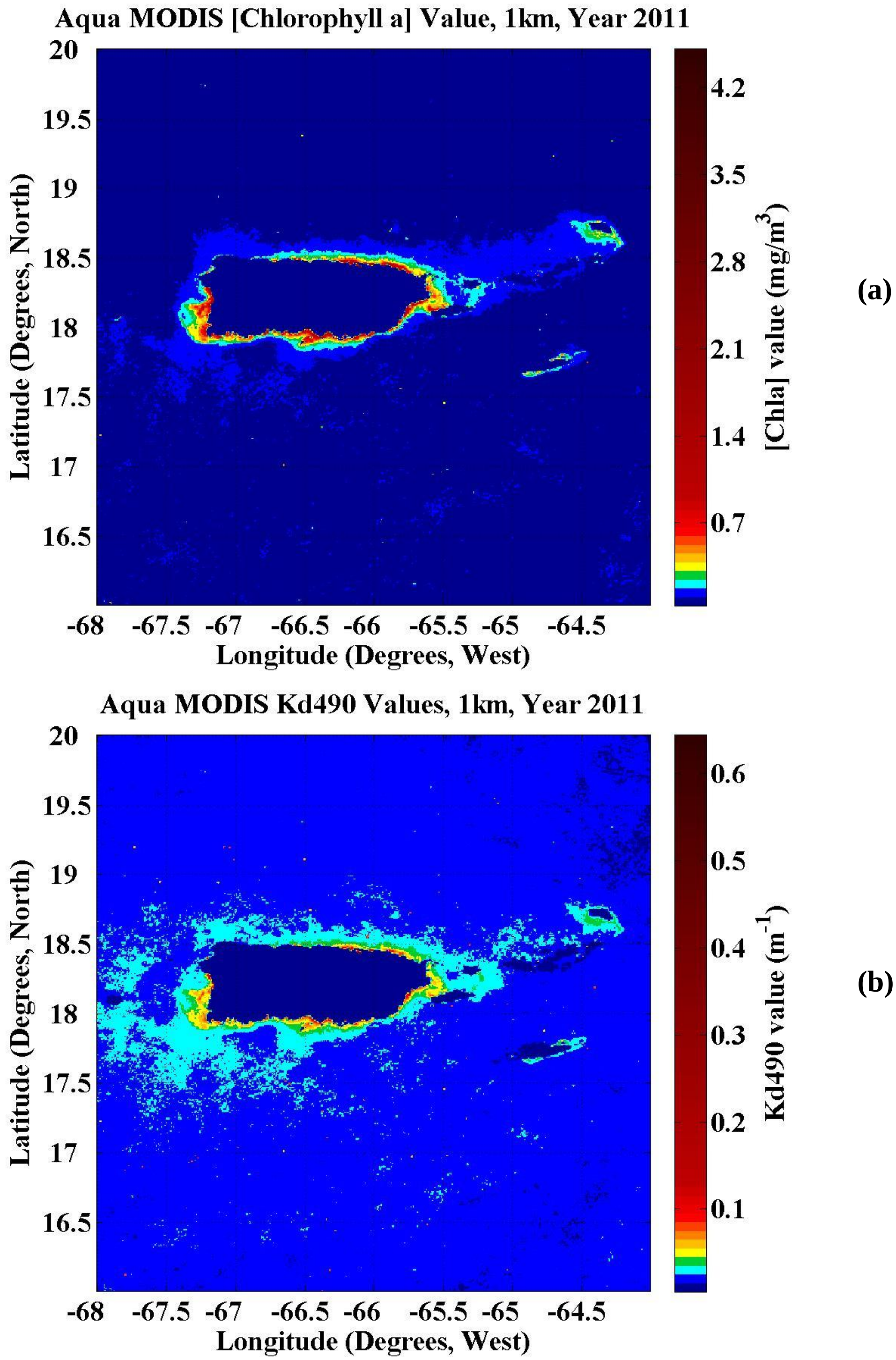

Figure 16. Study area image of Aqua MODIS [Chlorophyll a] value (a) and Kd490 (b) for 2011

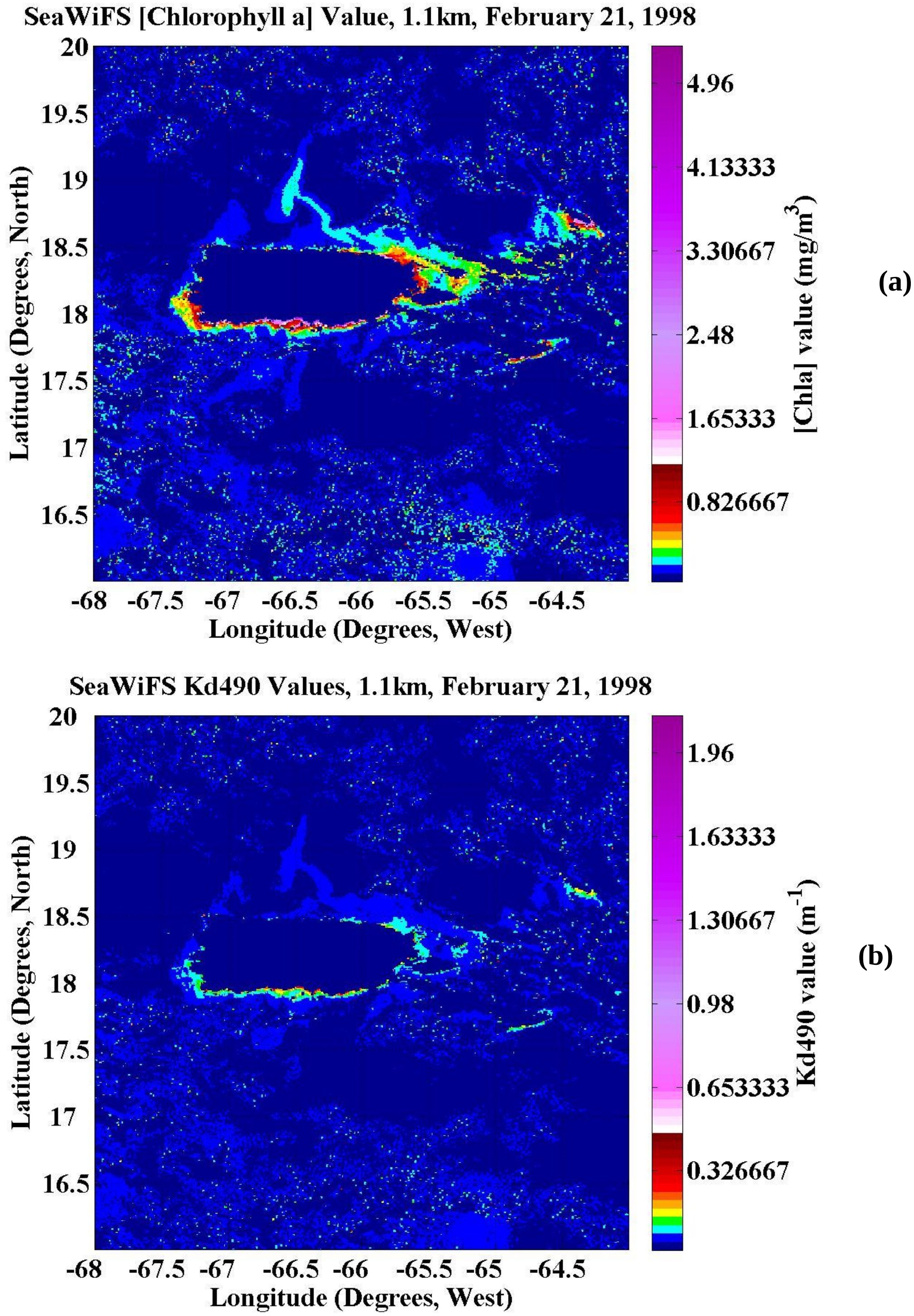

Figure 17. Study area image of SeaWiFS [Chlorophyll a] value (a) and Kd490 (b) for February 21, 1998

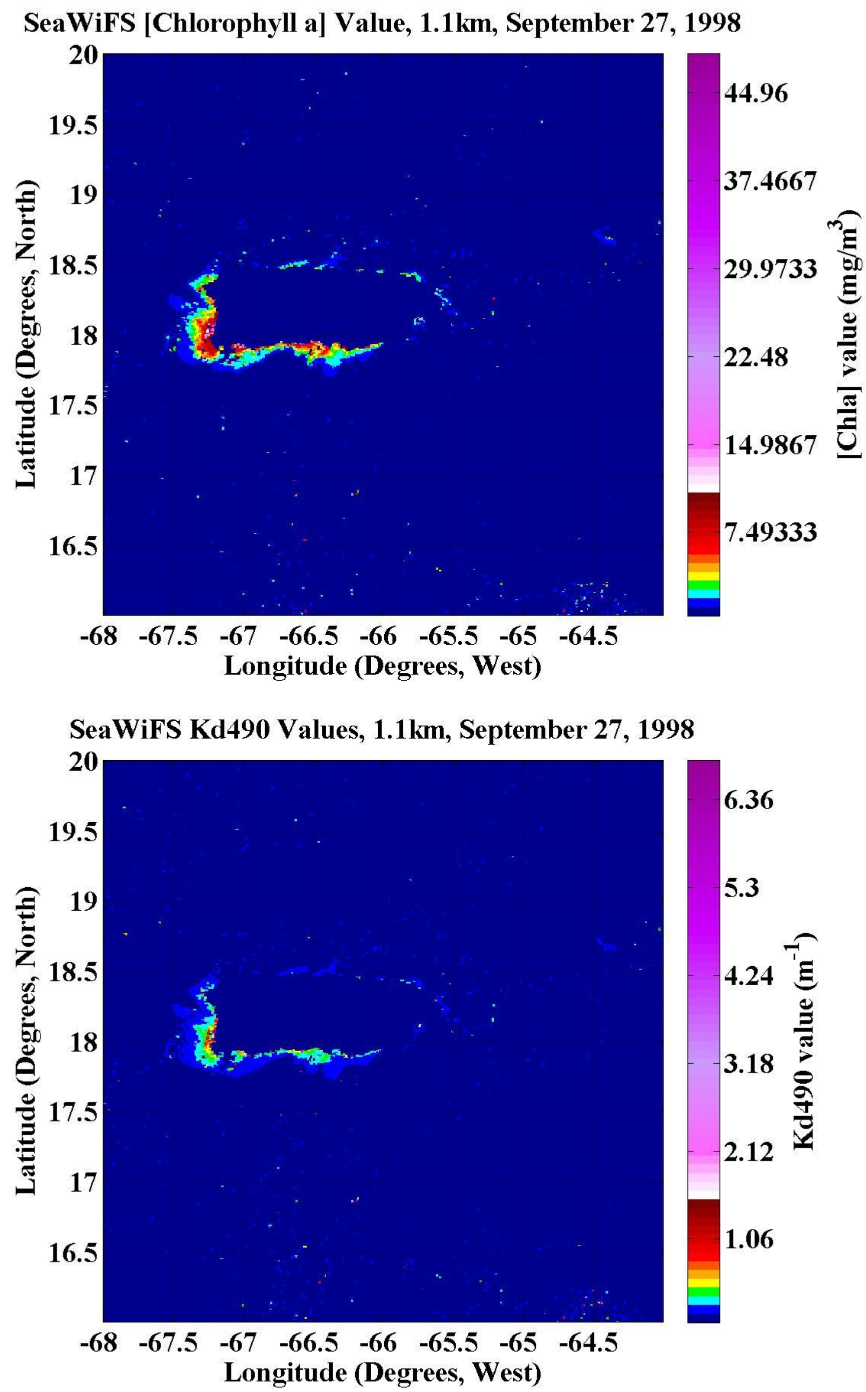

(a)

(b)

Figure 18. Study area image of SeaWiFS [Chlorophyll a] value (a) and Kd490 (b) for September 27, 1998

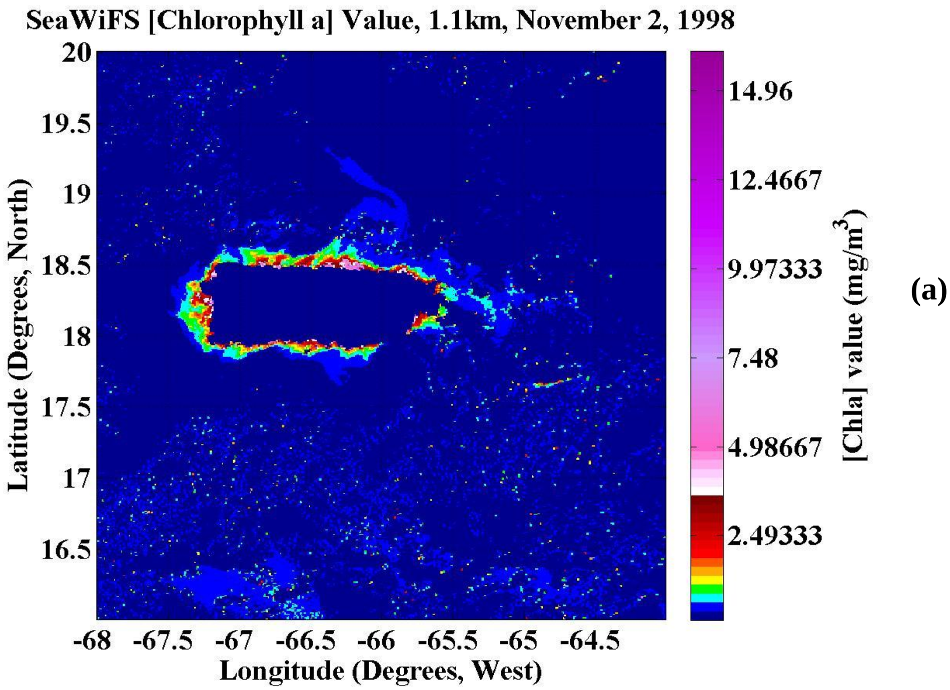

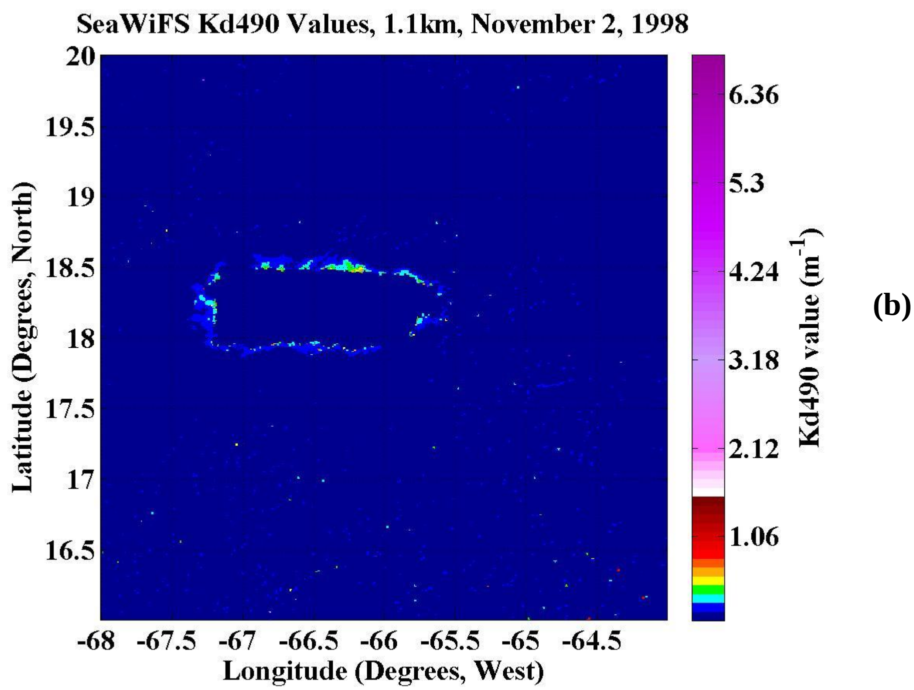

Figure 19. Study area image of SeaWiFS [Chlorophyll a] value (a) and Kd490 (b) for November 2, 1998

3.3 Pearson Correlation Coefficients

The critical value for the Pearson's correlation coefficient (*r*) at a level of significance of a two-tailed test, with a factor of 16 years multiplied by a factor of three rivers (*i.e.*, Western and Southern regions), it gave an N of 48, and therefore a degree of freedom of 47. A *p* value of 0.05 was selected, with a corresponding *r* equaled to 0.2816 and -0.2816. Similarly, for two rivers (*i.e.*, Eastern region) it gave an N of 32, and therefore a degree of freedom 31. A $p = 0.05$ value gave a corresponding *r* equaled to 0.3440 and -0.3440. Also, for four rivers (*i.e.*, Northern region), it gave an N of 64, and therefore a degree of freedom 63. A $p = 0.05$ value gave a corresponding *r* equaled to 0.2441 and -0.2441.

The [Chla] range of values (mg/m^3) was the following: 0 < Light < 1, 1 <= Moderate < 2, 2 <= High < 3, >= 3 Intense. The Kd490 range of values (m^{-1}) was the following: 0 < Light < 0.1, 0.1 <= Moderate < 0.2, 0.2 <= High < 0.3, >= 0.3 Intense. The river discharge range of values (ft^3/s) was the following: 0 < Light < 300, 300 <= Moderate < 600, 600 <= High < 900, >= 900 Intense.

3.3.1 Kd490 and [Chla] Relationships

The *r* for Kd490 and [Chla], at 2km from the river mouth, for 1998 to 2013 varied (Figure 19 and 20). For the annual relationship, the Western rivers (Figure 20a) showed a light to moderate Kd490 and [Chla], with a very strong increasing *r* (*i.e.*, 0.9203). The Northern rivers (Figure 20b) showed a low Kd490 and a low to moderate [Chla], with a very strong increasing *r* (*i.e.*, 0.9592). The Eastern rivers (Figure 20c) showed a low to moderate Kd490 and a low to moderate [Chla], with a strong increasing *r* (*i.e.*, -0.6297). The Southern rivers (Figure 20d) showed a low to high Kd490 and a low to moderate [Chla], with a strong increasing *r* (*i.e.*, 0.7635).

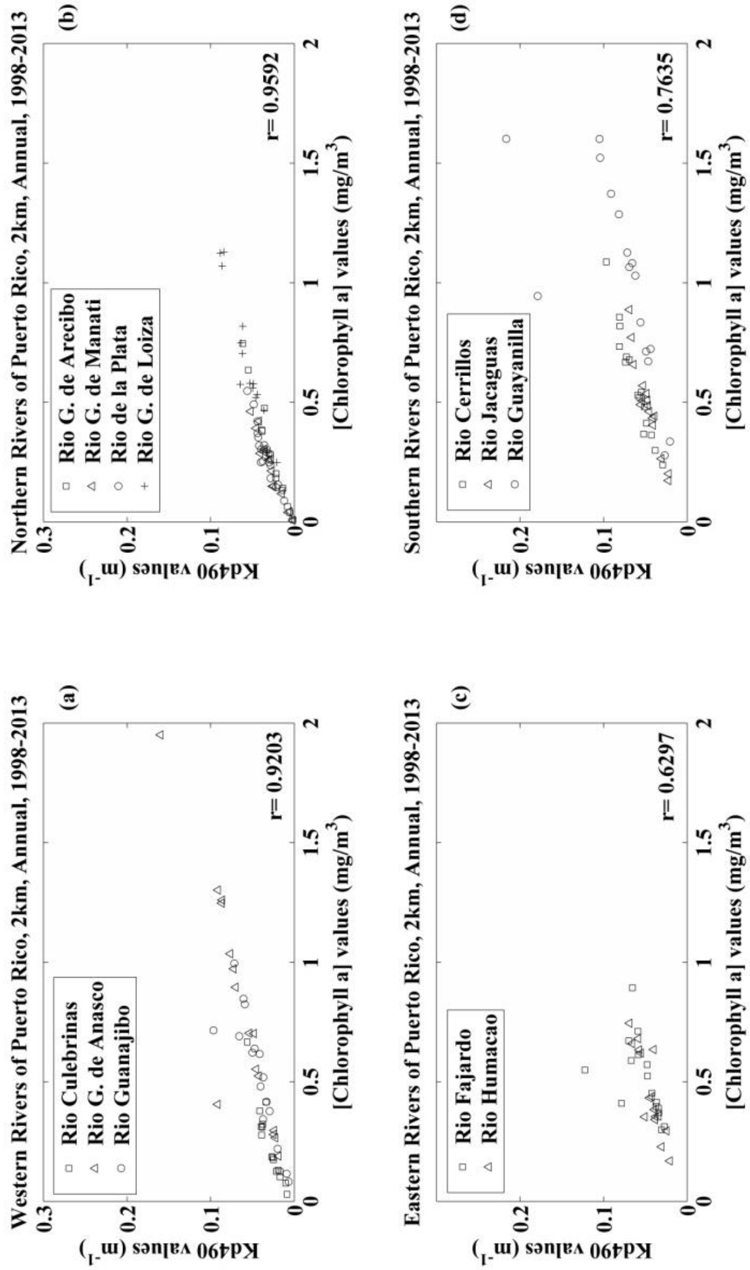

Figure 20. Kd490 and [Chla], annual mean values, of (a) Western Rivers, (b) Northern Rivers, (c) Eastern Rivers, and (d) Southern Rivers, 2km away from the river mouth, Puerto Rico, 1998-2013; **significant values**

During the rainy season, the *r* for Kd490 and [Chla], for 1998 to 2013 (Figure 21) were very similar to the annual *r*. The Western, Northern, and Southern rivers showed, respectively, a very strong increasing *r* (*i.e.*, 0.8792, 0.9532, and 0.7026). The Eastern rivers showed a strong increasing *r* (*i.e.*, 0.6519).

During the dry season, the *r* for Kd490 and [Chla], for 1998 to 2013 fluctuated (Figure 21). The Western, Northern, Eastern, and Southern rivers showed, respectively, a very strong increasing *r* (*i.e.*, 0.9683, 0.9664, 0.7499, and 0.8512).

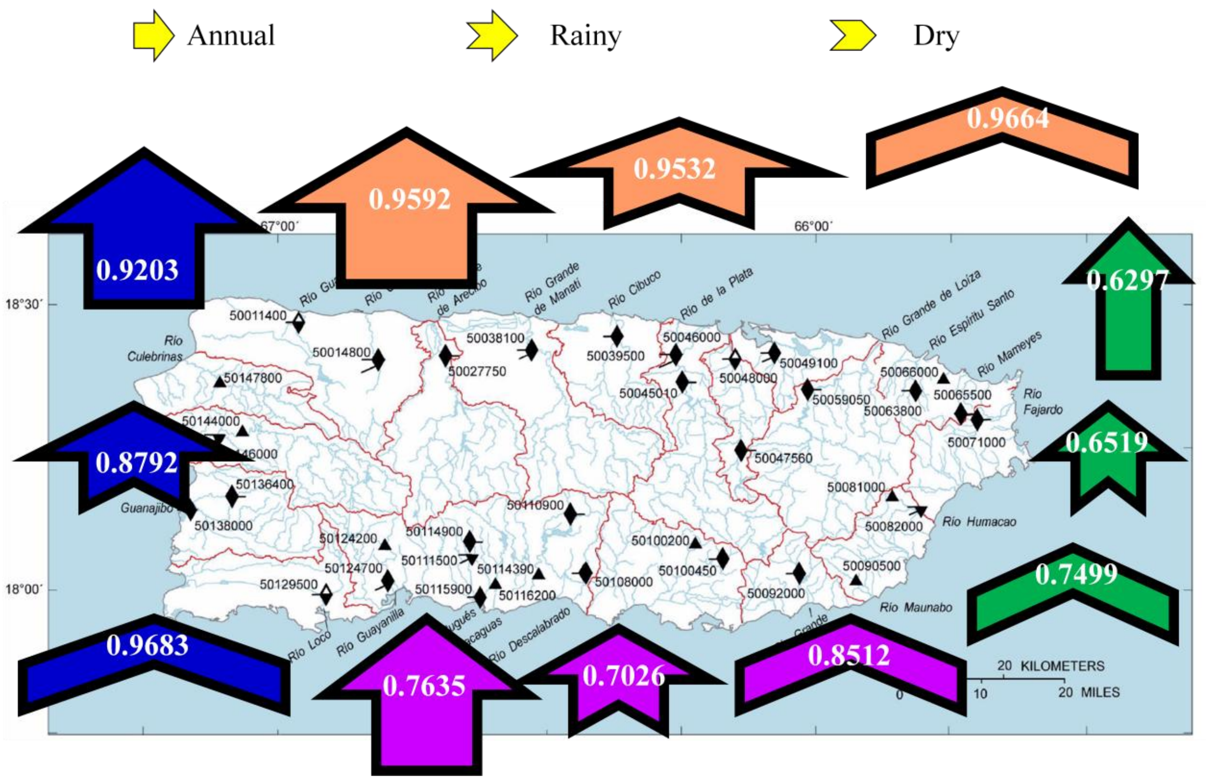

Figure 21. Correlation coefficients of Kd490 and [Chla], annual, rainy and dry seasons, 2km away from the river mouth, Puerto Rico, 1998-2013, **significant values**: North, df=63; West and South, df=47; East, df=31; $p < 0.05$

In summary, during the annual and seasonal periods, all the four regions Kd490 and [Chla] were statistically significant, in the following decreasing order: Northern, Western, Southern, and Eastern, but for the dry season where Western region was more significant than the Northern region. The dry season *r* were greater than rainy season ones. In addition, each rivers region exhibited a specific Kd490 and [Chla] pattern.

By analogy, annually (Table 3), from 3 to 16km away from the river mouth, the Southern region showed a very strong increasing *r* all along the distance. The Western region showed a very strong increasing *r*, but at 15km with a strong increasing *r*. The Eastern region showed a very strong increasing *r*, but at 5 to 7km with a strong increasing *r*. The Northern region showed a very strong increasing *r*, but at 4 and 12km with a strong increasing *r*, a moderate increasing *r* at 5km, and a weak increasing *r* at 7km. The stability of *r* among the regions was seen in the following decreasing order: Southern, Western, Eastern, and Northern region. For all the regions and at all the distances, the *r* were statistically significant, but at 7km for the Northern region.

Table 3. *Correlation coefficients of Kd490 and Chla, Annual, Puerto Rico, 1998 to 2013*

Distance	West	North	East	South
2km	**0.9203**	**0.9592**	**0.6297**	**0.7635**
3km	**0.8814**	**0.7896**	**0.9421**	**0.9238**
4km	**0.9695**	**0.4829**	**0.9586**	**0.9699**
5km	**0.9623**	**0.4129**	**0.3755**	**0.9459**
6km	**0.9609**	**0.5509**	**0.8440**	**0.9488**
7km	**0.9499**	0.2107	**0.9341**	**0.9720**
8km	**0.9460**	**0.8496**	**0.9463**	**0.7020**
9km	**0.9309**	**0.8216**	**0.9507**	**0.9570**
10km	**0.9274**	**0.9340**	**0.9451**	**0.9651**
11km	**0.9206**	**0.9257**	**0.8819**	**0.9605**
12km	**0.9460**	**0.5783**	**0.9404**	**0.9599**
13km	**0.9416**	**0.9450**	**0.7691**	**0.9686**
14km	**0.7817**	**0.9439**	**0.7446**	**0.9648**
15km	**0.5262**	**0.9308**	**0.9245**	**0.9662**
16km	**0.9246**	**0.9433**	**0.9191**	**0.9641**

Notes: **Significant values**, North, df=63; West and South, df=47; East, df=31; $p < 0.05$

During the rainy season (Table 4), from 3 to 16km away from the river mouth, the Southern and Western regions showed a very strong increasing *r*, all along the distance. The Eastern region showed a very strong increasing *r*, but at 6km, which showed a strong increasing *r*, and at 7km with a weak increasing *r*. The Northern region showed a very strong increasing *r*, but at 4 and 5km, which showed a moderate increasing *r*. Similarly to annual patterns, the stability of *r* among the regions was seen in the following decreasing order: Southern, Western, Eastern, and Northern region. For all the regions and at all the distances, the *r* were statistically significant.

Table 4. *Correlation coefficients of Kd490 and Chla, Rainy Season, Puerto Rico, 1998 to 2013*

Distance	West	North	East	South
2km	**0.8792**	**0.9532**	**0.6519**	**0.7026**
3km	**0.8158**	**0.7481**	**0.9337**	**0.9695**
4km	**0.9678**	**0.4036**	**0.9461**	**0.9622**
5km	**0.9564**	**0.3972**	**0.8838**	**0.9589**
6km	**0.9618**	**0.4835**	**0.8662**	**0.9463**
7km	**0.9548**	**0.4257**	**0.8925**	**0.9738**
8km	**0.9547**	**0.9359**	**0.9374**	**0.9577**
9km	**0.9439**	**0.7850**	**0.9549**	**0.9583**
10km	**0.9346**	**0.9528**	**0.9424**	**0.9678**
11km	**0.9077**	**0.9420**	**0.9316**	**0.9606**
12km	**0.9437**	**0.9605**	**0.9570**	**0.9616**
13km	**0.9280**	**0.9572**	**0.9404**	**0.9811**
14km	**0.9362**	**0.9563**	**0.9276**	**0.9812**
15km	**0.9216**	**0.9487**	**0.9347**	**0.9801**
16km	**0.9217**	**0.9401**	**0.8991**	**0.9725**

Notes: **Significant values**, North, df=63; West and South, df=47; East, df=31; $p < 0.05$

During the dry season (Table 5), from 3 to 16km away from the river mouth, the Southern and Eastern regions showed a very strong increasing *r*, respectively, but at 8km and 5km, which displayed a moderate increasing *r*. The Western region showed a very strong increasing *r*, but at 15km, which displayed a weak increasing *r*. The Northern region showed a very strong increasing *r*, but at 7km, which showed a slight decreasing *r*, and at 12km, which illustrated a slight increasing *r*. The stability of *r* among the regions was seen in the following decreasing order: Southern, Eastern, Western, and Northern region. For all the regions and at all the distances, the *r* were statistically significant, but at 15km for the Western region, 7km for the Northern region, and 5km for the Eastern region.

Table 5. *Correlation coefficients of Kd490 and Chla, Dry Season, Puerto Rico, 1998 to 2013*

Distance	West	North	East	South
2km	**0.9683**	**0.9664**	**0.7499**	**0.8512**
3km	**0.9420**	**0.8737**	**0.9667**	**0.8504**
4km	**0.9643**	**0.9513**	**0.9693**	**0.9472**
5km	**0.9583**	**0.9333**	0.0566	**0.8795**
6km	**0.9561**	**0.9237**	**0.8658**	**0.9323**
7km	**0.9414**	-0.0242	**0.9544**	**0.8956**
8km	**0.9275**	**0.8366**	**0.9537**	**0.3219**
9km	**0.9168**	**0.9297**	**0.9479**	**0.9342**
10km	**0.9096**	**0.8872**	**0.9557**	**0.9273**
11km	**0.9173**	**0.8662**	**0.8374**	**0.9353**
12km	**0.9527**	**0.2982**	**0.9034**	**0.9327**
13km	**0.9443**	**0.8785**	**0.6897**	**0.9117**
14km	**0.9225**	**0.8269**	**0.7027**	**0.9215**
15km	0.2612	**0.8908**	**0.9259**	**0.9387**
16km	**0.9187**	**0.8990**	**0.9161**	**0.9488**

Notes: **Significant values**, North, df=63; West and South, df=47; East, df=31; $p < 0.05$

3.3.2 Kd490 and river discharge relationships

The *r* for Kd490 and river discharge, at 2km from the river mouth, for 1998 to 2013 varied (Figure 23). During the annual period, the Western rivers (Figure 22a) showed a light to moderate Kd490 and a low to high river discharge, with a weak increasing *r* (*i.e.*, 0.2775). The Northern rivers (Figure 22b) showed a low Kd490 and a low to intense river discharge, with a

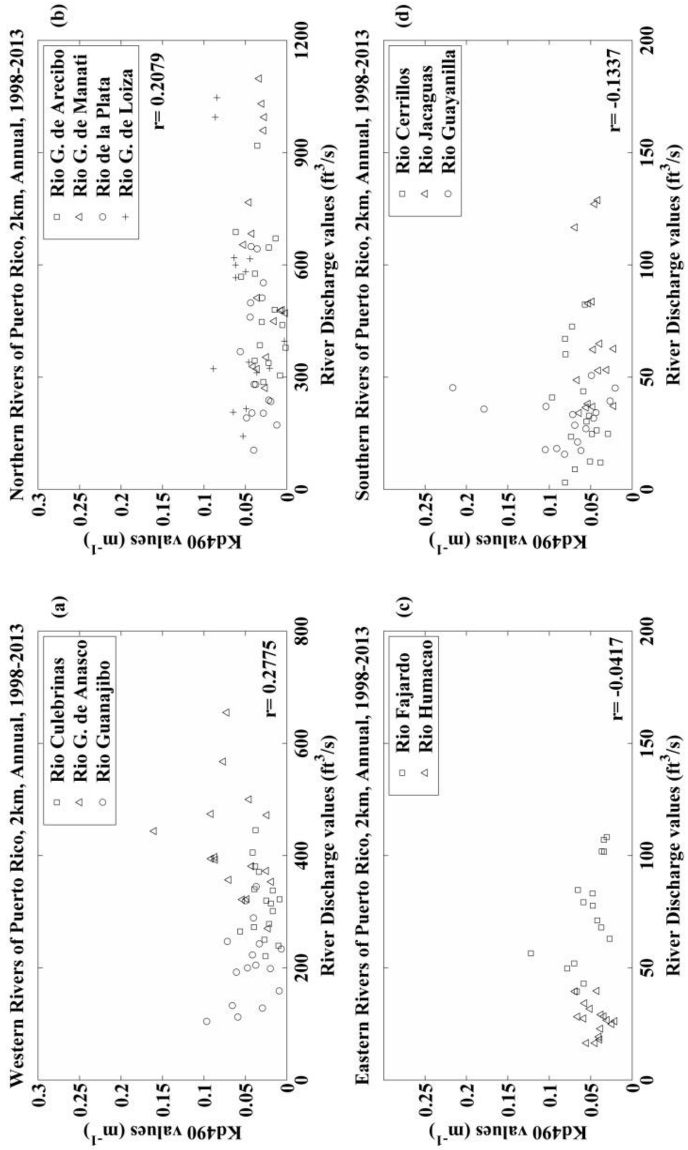

Figure 22. Kd490 and river discharge, annual mean values, of (a) Western Rivers, (b) Northern Rivers, (c) Eastern Rivers, and (d) Southern Rivers, 2km away from the river mouth, Puerto Rico, 1998-2013; **significant values**

weak increasing *r* (*i.e.*, 0.2079). The Eastern rivers (Figure 22c) showed a low to moderate Kd490 and a low river discharge, with a slight decreasing *r* (*i.e.*, -0.0417).The Southern rivers (Figure 22d) showed a low to moderate Kd490 and a low river discharge, with a slight decreasing *r* (*i.e.*, -0.1337).

During the rainy season, the *r* for Kd490 and river discharge, for 1998 to 2013 (Figure 23) were very similar to the annual *r*. The Western rivers showed a weak increasing *r* (*i.e.*, 0.2011). The Northern rivers showed a moderate increasing *r* (*i.e.*, 0.3513). The Eastern and Southern rivers showed, respectively, a slight decreasing *r* (*i.e.*, -0.0888 and -0.0557).

During the dry season, the *r* for Kd490 and river discharge, for 1998 to 2013 fluctuated (Figure 23). The Western rivers showed a weak increasing *r* (*i.e.*, 0.2616). The Northern rivers showed a slight decreasing *r* (*i.e.*, -0.1219). The Eastern rivers showed a slight increasing *r* (*i.e.*, 0.0197). The Southern rivers showed a weak decreasing *r* (*i.e.*, -0.2456).

In summary, only during the rainy season, the Northern rivers region Kd490 and river discharge were statistically significant. However, each rivers region exhibited a specific Kd490 and river discharge pattern.

By analogy, annually (Table 6), from 3 to 16km away from the river mouth, for all the regions, they displayed slight to weak increasing and decreasing *r*, specifically for the Southern region. However, the Eastern region showed a moderate to strong increasing *r*, which was statistically significant near 3km and midway along the distance. The Northern and Western regions showed weak to moderate decreasing *r*, which were statistically significant away from the river mouth and midway, but only away from the river mouth for the Western region.

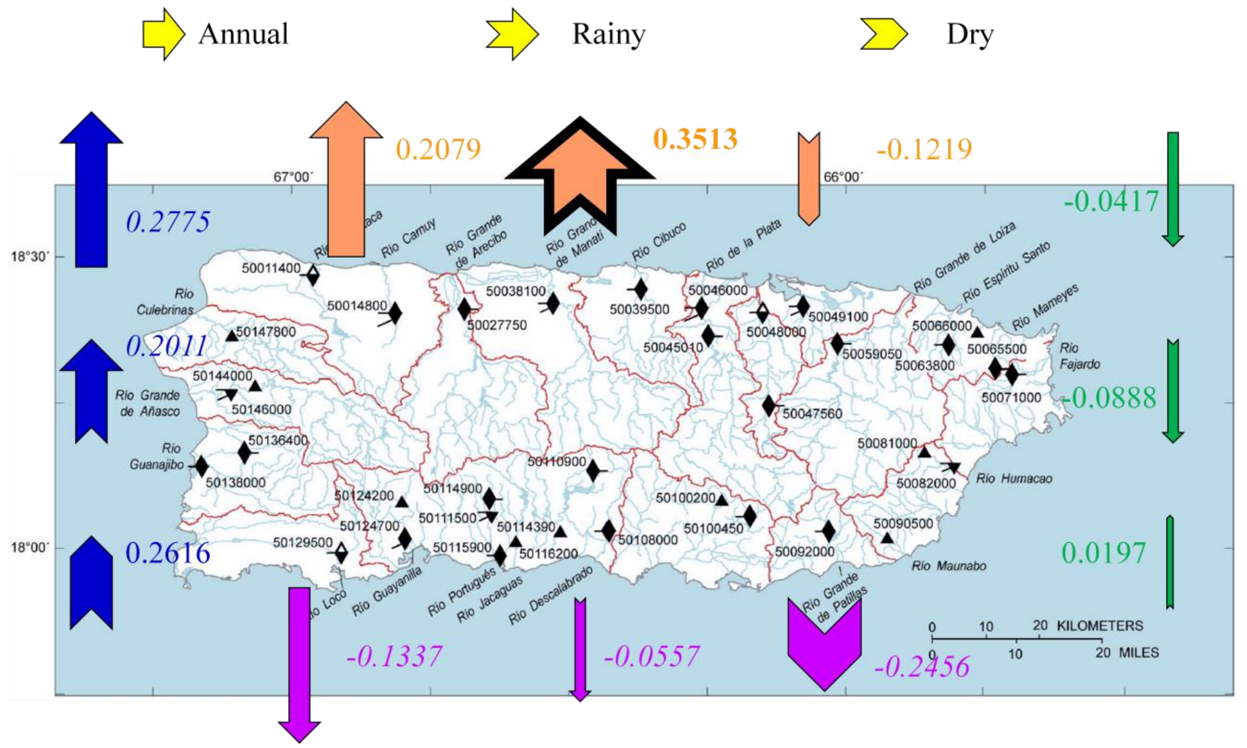

Figure 23. Correlation coefficients of Kd490 and river discharge, annual, rainy and dry seasons, 2km away from the river mouth, Puerto Rico, 1998-2013, **significant values**: North, df=63; West and South, df=47; East, df=31; $p < 0.05$

During the rainy season (Table 7), from 3 to 16km away from the river mouth, for all the regions, they displayed slight to weak increasing and decreasing *r*, especially for the Southern region, similar to the annual patterns. However, the Eastern and Western regions showed moderate to strong increasing *r*, which were statistically significant near 3km from the river mouth. The Northern region showed weak to moderate decreasing *r*, which were statistically significant away from the river mouth.

Table 6. *Correlation coefficients of Kd490 and River Discharge, Annual, Puerto Rico, 1998 to 2013*

Distance	West	North	East	South
2km	0.2775	0.2079	-0.0417	-0.1337
3km	0.0665	0.0641	**0.4658**	-0.1531
4km	0.1373	-0.0874	**0.6302**	-0.1012
5km	0.0077	-0.0973	-0.1370	-0.0457
6km	-0.1093	-0.1523	**0.3899**	0.2701
7km	-0.0568	-0.1786	**0.5509**	0.1020
8km	-0.0352	-0.1395	**0.4072**	0.0672
9km	-0.0294	**-0.2533**	**0.4431**	0.1802
10km	-0.0873	-0.2389	**0.3970**	0.1014
11km	-0.1425	**-0.2895**	0.2213	0.1005
12km	-0.2435	-0.0792	0.2173	0.0485
13km	**-0.2910**	-0.2436	0.2478	0.0282
14km	**-0.3334**	**-0.2475**	0.1979	0.0003
15km	-0.0741	**-0.2526**	0.1853	0.0146
16km	-0.2358	**-0.3103**	0.1769	-0.0591

Notes: **Significant values**, North, df=63; West and South, df=47; East, df=31; $p < 0.05$

During the dry season (Table 8), from 3 to 16km away from the river mouth, for all the regions, they displayed slight to weak increasing and decreasing *r*, especially for the Southern and Northern regions; the Eastern region included some moderate increasing *r*. However, the Eastern region showed moderate to strong increasing *r*, which were statistically significant along the distance. To the contrary, the Western region showed moderate to strong decreasing *r*, which was statistically significant along the distance.

Table 7. *Correlation coefficients of Kd490 and River Discharge, Rainy Season, Puerto Rico, 1998 to 2013*

Distance	West	North	East	South
2km	0.2011	**0.3513**	-0.0888	-0.0557
3km	0.1672	0.1687	0.2769	-0.0694
4km	**0.4346**	-0.0496	**0.4201**	0.0815
5km	**0.3884**	-0.0409	0.0023	0.0507
6km	0.2270	-0.0091	0.2561	0.2627
7km	0.2292	0.0403	**0.3595**	0.1053
8km	0.2602	-0.0444	0.3019	0.1851
9km	0.2318	-0.1255	0.1943	0.1735
10km	0.1870	-0.1275	0.0573	0.0784
11km	0.1596	-0.2153	0.0868	0.0899
12km	0.0809	-0.1896	0.0448	0.0637
13km	0.0240	-0.1965	0.0698	0.0763
14km	0.0436	-0.2276	0.0303	0.0157
15km	0.1071	**-0.2815**	0.0080	-0.0059
16km	0.0056	**-0.3146**	-0.0162	-0.0567

Notes: **Significant values**, North, df=63; West and South, df=47; East, df=31; $p < 0.05$

3.3.3 [Chla] and river discharge relationships

The *r* for [Chla] and river discharge, at 2km from the river mouth, for 1998 to 2013 varied (Figure 25). In the annual *r*, the Western rivers (Figure 24a) showed a light to moderate [Chla] and a low to high river discharge, with a weak increasing *r* (*i.e.*, 0.2750). The Northern rivers (Figure 24b) showed a low to moderate [Chla] and a low to intense river discharge, with a weak increasing *r* (*i.e.*, 0.2752). The Eastern rivers (Figure 24c) showed a low [Chla] and river discharge, with a slight increasing *r* (*i.e.*, 0.0410). The Southern rivers (Figure 24d) showed a low to moderate [Chla] and a low river discharge, with a weak decreasing *r* (*i.e.*, -0.2176).

Table 8. *Correlation coefficients of Kd490 and River Discharge, Dry Season, Puerto Rico, 1998 to 2013*

Distance	West	North	East	South
2km	0.2616	-0.1219	0.0197	-0.2456
3km	-0.0264	-0.0327	**<u>0.4956</u>**	-0.1650
4km	-0.1513	0.0506	**<u>0.5558</u>**	-0.2551
5km	-0.2677	0.1744	-0.1955	-0.1945
6km	**<u>-0.3370</u>**	0.0224	0.2230	0.1320
7km	**<u>-0.3212</u>**	-0.1640	**<u>0.5157</u>**	0.1471
8km	**<u>-0.3705</u>**	0.0508	**<u>0.5332</u>**	0.0208
9km	-0.2511	0.0273	**<u>0.5223</u>**	0.1988
10km	-0.2506	-0.0780	**<u>0.5130</u>**	0.1552
11km	**<u>-0.3063</u>**	-0.1190	**<u>0.4584</u>**	0.0584
12km	**<u>-0.3783</u>**	0.1373	**<u>0.3748</u>**	-0.0964
13km	**<u>-0.4222</u>**	-0.1120	0.3358	-0.1791
14km	**<u>-0.3309</u>**	0.1271	0.2242	0.0298
15km	-0.1458	-0.1255	**<u>0.3663</u>**	0.0071
16km	**<u>-0.3389</u>**	-0.1462	0.3320	-0.0591

Notes: **<u>Significant values</u>**, North, df=63; West and South, df=47; East, df=31; $p < 0.05$

During the rainy season, the *r* for [Chla] and river discharge, for 1998 to 2013 varied (Figure 25). In the annual *r*, the Western rivers showed a weak increasing *r* (*i.e.*, 0.2488). The Northern rivers showed a strong increasing *r* (*i.e.*, 0.4588). The Eastern and Southern rivers showed, respectively, a slight decreasing *r* (*i.e.*, -0.0022 and -0.0941).

During the dry season, the *r* for [Chla] and river discharge, for 1998 to 2013 fluctuated (Figure 25). In the annual *r*, the Western rivers showed a weak increasing *r* (*i.e.*, 0.2551). The Northern rivers showed a slight decreasing *r* (*i.e.*, -0.1229). The Eastern rivers showed a strong increasing *r* (*i.e.*, 0.4490). The Southern rivers showed a weak decreasing *r* (*i.e.*, -0.2809).

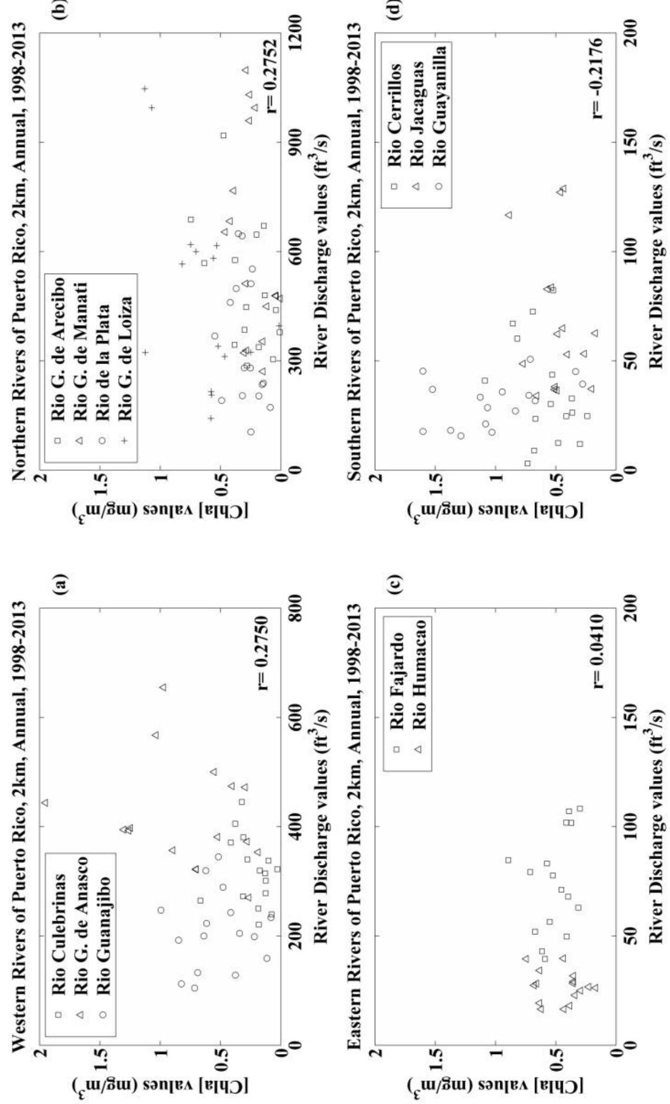

Figure 24. [Chla] and river discharge, annual mean values, of (a) Western Rivers, (b) Northern Rivers, (c) Eastern Rivers, and (d) Southern Rivers, 2km away from the river mouth, Puerto Rico, 1998-2013; **significant values**

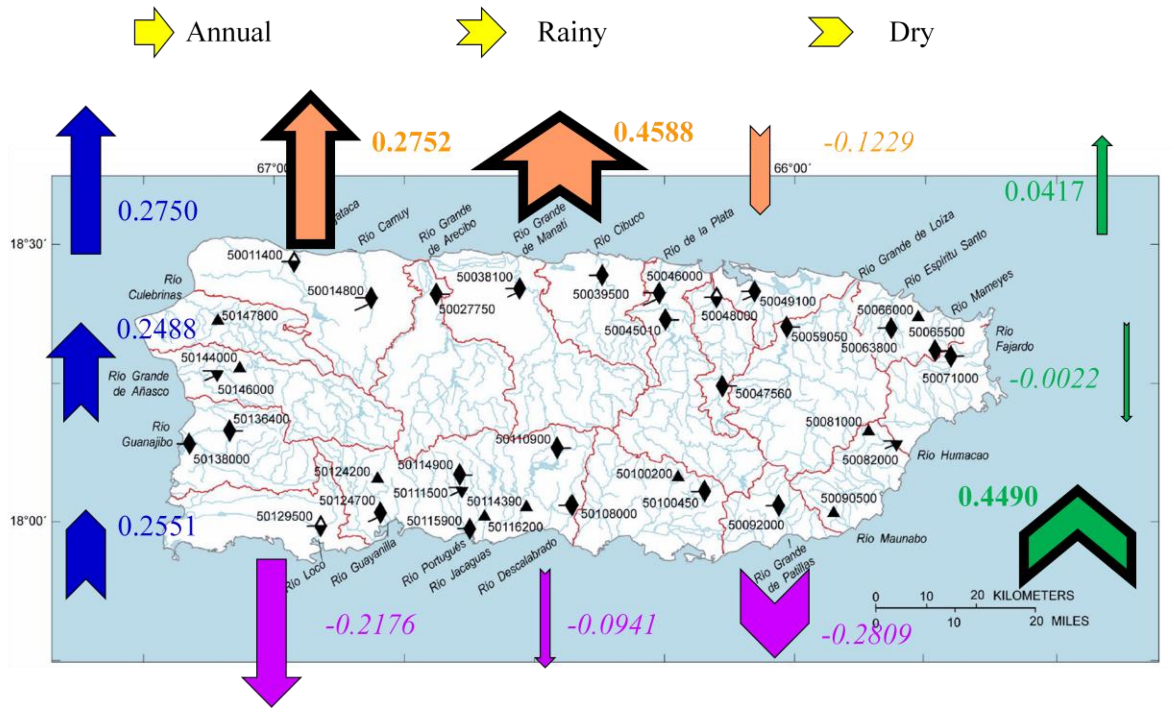

Figure 25. Correlation coefficients of [Chla] and river discharge, annual, rainy and dry seasons, 2km away from the river mouth, Puerto Rico, 1998-2013, **significant values**: North, df=63; West and South, df=47; East, df=31; $p < 0.05$

In summary, during the annual and rainy season, the Northern rivers region and during the dry season, the Eastern region [Chla] and river discharge were statistically significant. However, each rivers region exhibited a specific [Chla] and river discharge pattern.

By analogy, annually (Table 9), from 3 to 16km away from the river mouth, for all the regions, they displayed slight to weak increasing and decreasing *r*, specifically for the Southern region. However, the Eastern region showed a moderate to strong increasing *r*, which were statistically significant near 3km and midway along the distance. The Northern and Western regions showed weak to moderate decreasing *r*, which were statistically significant away from the river mouth for both regions, but only midway, for the Northern region.

Table 9. *Correlation coefficients of [Chla] and River Discharge, Annual, Puerto Rico, 1998 to 2013*

Distance	West	North	East	South
2km	0.2750	**0.2752**	0.0410	-0.2176
3km	0.0769	0.0664	**0.5915**	-0.2155
4km	0.1409	0.0840	**0.7354**	-0.1808
5km	-0.0055	0.0628	**0.4755**	-0.1038
6km	-0.1900	-0.0688	**0.6842**	**0.3114**
7km	-0.1093	-0.0827	**0.6806**	0.1355
8km	-0.0843	0.0272	**0.5997**	0.2085
9km	-0.0913	-0.0832	**0.6160**	0.1801
10km	-0.1812	-0.1051	**0.6019**	0.1455
11km	-0.2809	-0.1289	0.3119	0.1166
12km	**-0.3398**	-0.0909	**0.4487**	0.0638
13km	**-0.4044**	-0.1414	0.2979	0.0287
14km	**-0.3522**	-0.1487	0.2522	-0.0212
15km	**-0.3644**	-0.1663	**0.4043**	-0.0078
16km	**-0.4002**	-0.2250	**0.3794**	-0.0571

Notes: **Significant values**, North, df=63; West and South, df=47; East, df=31; $p < 0.05$

During the rainy season (Table 10), from 3 to 16km away from the river mouth, for all the regions, they displayed slight to weak increasing and decreasing *r*, especially for the Northern region; the Eastern region included some moderate increasing *r*. However, the Eastern region showed moderate to strong increasing *r*, which were statistically significant near 3km from the river mouth, and midway along the distance. The Western region showed strong increasing *r*, which were statistically significant near 3km from the river mouth. The Southern region showed moderate increasing *r*, which was statistically significant near midway along the distance.

Table 10. *Correlation coefficients of [Chla] and River Discharge, Rainy Season, Puerto Rico, 1998 to 2013*

Distance	West	North	East	South
2km	0.2488	**0.4588**	-0.0022	-0.0941
3km	0.2635	0.1796	**0.4170**	-0.0287
4km	**0.4583**	0.1591	**0.5689**	-0.0107
5km	**0.4118**	0.1996	0.2991	0.0134
6km	0.2084	0.0733	**0.5250**	**0.3187**
7km	0.2275	0.0390	**0.5326**	0.1571
8km	0.2462	0.0972	**0.5037**	0.2318
9km	0.2290	0.0280	**0.3549**	0.1766
10km	0.1472	-0.0092	0.2878	0.1292
11km	0.0563	-0.0783	0.3364	0.1036
12km	0.0106	-0.0975	0.2320	0.0661
13km	-0.0780	-0.1244	0.2824	0.0505
14km	-0.0620	-0.1589	0.2667	-0.0189
15km	-0.0166	-0.2045	0.1378	-0.0344
16km	-0.1148	-0.2322	0.1081	-0.0697

During the dry season (Table 11), from 3 to 16km away from the river mouth, for all the regions, they displayed slight to weak increasing and decreasing *r*, especially for the Northern region. However, the Eastern region showed strong increasing *r*, which were statistically significant along the distance. To the contrary, the Western region showed moderate to strong decreasing *r*, which were statistically significant along the distance.

Table 11. *Correlation coefficients of [Chla] and River Discharge, Dry Season, Puerto Rico, 1998 to 2013*

Distance	West	North	East	South
2km	0.2551	-0.1229	**0.4490**	-0.2809
3km	-0.1517	0.0210	**0.5551**	**-0.2975**
4km	-0.2020	0.0526	**0.5873**	-0.2672
5km	**-0.3405**	0.1372	**0.4845**	-0.2001
6km	**-0.4314**	0.0595	**0.5031**	0.1385
7km	**-0.4047**	0.0492	**0.6572**	0.1357
8km	**-0.4646**	0.0750	**0.6672**	0.1265
9km	**-0.3688**	0.0928	**0.6673**	0.2079
10km	**-0.3927**	0.0404	**0.6328**	0.2032
11km	**-0.4579**	0.0442	**0.4632**	0.0844
12km	**-0.4751**	0.0745	**0.5889**	-0.0562
13km	**-0.5096**	0.0372	0.2171	-0.1748
14km	-0.2007	0.0498	0.1609	0.0416
15km	**-0.5201**	-0.0221	**0.5801**	0.0297
16km	**-0.4845**	-0.0395	**0.5451**	-0.0395

4 DISCUSSION

There are several factors that could explain the seasonal and regional variations in the [Chla], Kd490, and river discharge data and their relationships during the study period for the coastal waters of Puerto Rico. Some of these factors were climate, sediment types, wave energy, and shelf topography.

The Western rivers region is part of the leeward side of Puerto Rico. It is partially sheltered from the prevailing winds by the elevation of the central mountain range and is drier due to the rain shadow effect. The Southwestern coast has low wave energy and displays carbonate clastic (*i.e.*, carbonate, inorganic) shelf sediments, which is mostly of biogenic. The turbidity of the water is less influenced by the river discharges of the main rivers than by the wind resuspension of bottom sediments. Due to the Easterly trade winds in combination with diurnal land-sea breeze, the Western region displays a rainfall increase (Warne, Webb, and Larsen, 2005). This region is influenced by strong Mona tidal currents (Morelock *et al.*, 2000). The Western shelf inclination varies from 0.1 to 0.5^o, and its broad width varies from 0.4 to 6.6km (Morelock *et al.*, 2000).

The Southern rivers region, being part of the leeward side of Puerto Rico, not only exhibits the same characteristics as the Western rivers region, but also displays the similar shelf sediment types and wave energy, but more affected by the rain shadow effect than in the Western rivers region. The mean annual rainfall in the Southern coast is lower than the evapotranspiration rate, and has weak currents (Warne, Webb, and Larsen, 2005). The Southern shelf inclination varies from 0.1 to 0.7^o, a bit more inclined than the Western one, and its broader width varies from 5 to 21km (Morelock *et al.*, 2000).

The Northern rivers region is part of the windward side of Puerto Rico. The Northern region is more affected by the prevailing Eastern trade winds and therefore is the rainier side of the island. The Northern coast displays mostly terrigenous with carbonate clastic shelf sediments. It has the highest wave energy and strong currents (Warne, Webb, and Larsen, 2005). The Northern shelf has the steepest inclination, which varies from 0.22 to 11^o, and its narrow shelf varies from 0.3 to 3.2km (Morelock *et al.*, 2000).

The Eastern rivers region is also part of the windward side of Puerto Rico, influenced by the same characteristics as the Northern rivers region. However, it has carbonate clastic shelf sediments, lower wave energy, and a broad insular shelf (Warne, Webb, and Larsen, 2005). It has the smallest watersheds, with steep gradients from the mountain, and much steeper gradients from El Yunque rain forest than the Northern region. The river stations are located in the steep parts (Díaz, *et al.*, 1998). In addition, it is influenced by El Yunque rain forest vegetation, has enhanced trapping of sediments and associated nutrients. The Eastern rivers exhibit a lower river discharge and shows evidence of a well mixed – unstratified estuary (Brown *et al.*, 2008). The Eastern shelf is the least inclined, varying from 0.1 to 0.3^{o}, and its widest width varies from 0.5 to 65km (Morelock *et al.*, 2000).

4.1 [Chla] and Kd490

There was a regional variation in [Chla] and Kd490 levels. This could be due to landscape and coastlines heterogeneity, which might have affected phytoplankton communities at different temporal and spatial scales (Gilbes, López, and Yoshioka, 1996).

4.2 River Discharge

There was a regional decreasing trend in river discharge and seasonal variation. Warne, Webb, and Larsen (2005) stated that in Puerto Rico, river discharge and watershed size were not strongly related. However, the centerline of the Cordillera Central, being 11km south of the center of the island, could influence the regional distribution of runoff and rainfall, due to the shape of the island. From Figure 1 and the Google topography map, the following can be inferred: the Western region has longer than wider rectangular steep gradient watersheds, and a multitude of tributaries. However, near and around the river station and towards the river mouth, the land is a flat plain. The Southern region has long, narrow, and very steep gradient watersheds, less tributaries, and river stations located in the steeper part. The Northern region has the largest watersheds, with steep gradients from the mountain, and a multitude of tributaries.

However, near and around the river station and towards the river mouth, the land is a flat plain and is very narrow. The Eastern region has the smallest watersheds with steep gradients from the mountain, and much steeper gradients from El Yunque rain forest than the Northern region, and low tributaries. The river stations are located in the steep parts (Díaz, *et al.*, 1998).

Another reason that could explain the regional variability in river discharge would be the estuary/river type for the four river regions. In accordance with Brown *et al.* (2008), and given the four river regions characteristics, the Western rivers exhibited low to high river discharge and showed evidence of a partially mixed – moderately stratified estuary. The Southern rivers also exhibited characteristics of a well mixed – unstratified estuary, however, with a negative estuarine circulation, and with a much lower river discharge. The Northern rivers exhibited higher river discharge, showed evidence of a salt wedge and well-stratified estuary. The Eastern rivers exhibited a lower river discharge, showed evidence of a well mixed – unstratified estuary (Brown *et al.*, 2008).

The seasonal latitudinal migration of the Intertropical Convergence Zone (ITCZ) distinguished the rainy season from the dry season. During the summer, the ITCZ is closer to the Northern Equatorial region, whereas, during the winter it is closer to the Southern Equatorial region (Brown *et al.*, 2007).

The difference in temporal consistency (*i.e.*, Western and Southern rivers), and non consistency patterns (*i.e.*, Northern and Eastern rivers) of river discharge, in this study, can also be explained by orographic precipitation (Warne, Webb, and Larsen, 2005). The more the vegetation, the less erosion and river runoff, such as El Yunque rain forest influence on the Eastern rivers (Brown *et al.*, 2008).

The decreasing river discharge trend observed during the rainy season could be likely due to less frequent and intense rainfall events, which could be enhanced by El Niño events. On the contrary, there was an increasing trend in river discharge over time during the dry season. This could be from more frequent and intense rainfall, which could be enhanced by La Niña events (*http://www.cpc.noaa.gov/products/analysis_monitoring/ensostuff/ensoyears.shtml*). El Niño increases tropical cyclone activity in the Equatorial Pacific, whereas it limits the North Atlantic hurricane activity, resulting in less rain. On the other hand, La Niña occurs with cooler sea surface temperature (SST) in the Equatorial Eastern Central Pacific and a low pressure in the Western and a high pressure in the Eastern Pacific. As, a result, it forms less cyclones in the Pacific and stronger hurricanes in the North Atlantic, resulting in more rain (Brown *et al.*, 2007).

4.3 Images of [Chla] and Kd490

The intensities and frequencies of short-term weather disturbances (*i.e.*, episodic events) that occurred during a specific year were highly variable. Several episodes were responsible for the major river discharge peaks observed during 1998, 2005, and 2011. In 1998, two intense episodic rainfall events, Hurricane Bonnie and Georges directly impacted Puerto Rico. In 2011, three intense episodic rainfall events, Tropical storms Emily and Maria passed near Puerto Rico, and Hurricane Irene passed through Puerto Rico. In 2005, no major events directly passed through or near Puerto Rico (*http://www.nhc.noaa.gov/data/tcr/index.php?basin=atl*).

El Niño was mostly likely responsible for low hurricane activities in the North Atlantic (Brown *et al.*, 2007). ENSO events occurred in 1997-1998, 2002-2003, 2003-2004, 2004-2005, 2006-2007, 2009-2010), while La Niña (*i.e.*, high hurricane activities in the North Atlantic) events occurred in 1998-2001, 2007-2009, 2010-2011 (*http://www.cpc.noaa.gov/products/analysis_monitoring/ensostuff/ensoyears.shtml*). The episodic events of 1998 and 2011 occurred during La Niña years. In 1998, the more intense [Chla] and Kd490 values, compared to 2011, were mostly due to the significant impacts of Hurricane Georges, the last major hurricane to affect Puerto Rico (Gilbes *et al.*, 2001).

The spatial variations observed in the [Chla] and of Kd490 images could be explained by temporal variations (*e.g.*, ocean circulation). Water motion (*e.g.*, eddies, El Niño, hurricanes) and ocean circulation can be explained by the pattern of planktonic distribution (Miller, 2004), which wander with flexible adaptivity (Miller, 2004).

4.4 Pearson correlation of Kd490 and [Chla] at 2km from the river mouth and along the shelf

Kd490 and [Chla] were strongly correlated in all the regions at 2km from the river mouth. High [Chla] might be related to high Kd490 because lower productivity could be reduced due elevated non-biogenic (*i.e.*, terrigenous) matter (Kirk, 2011). According to García-Sais, Williams, and Amirrezvani (in review) [Chla] could be very strongly correlated to Kd490, in comparison to non-biogenic sediments, at coral reef sites in coastal waters of Puerto Rico. In addition, along the insular shelf, from 3km to 16km the correlation between Kd490 and [Chla] was also statistically significant. Therefore, [Chla] seemed to be the main component which influenced turbidity in coastal waters of Puerto Rico during this 16-year period.

The r varied because turbidity and chlorophyll maxima were not always at 2km from the river mouth but close to it and with regional heterogeneity. Based on the works of Morelock *et al.* (2000), this regional heterogeneity could be explained by the shelf width in combination with ocean current; the Northern and Western regions have narrower insular shelves and stronger currents, which could generate greater resuspension of sediments in comparison to the Eastern and Southern regions.

The fact that in the inner shelf, the dry season [Chla] and Kd490 *r* were better correlated than to the rainy season could be explained by the fact that during the dry season, winter frontal storms increases runoff and brings high sediments to the entire shelf, whereas in the rainy season, tropical storms and hurricanes enhances runoff with higher sediments but only to the inner and middle shelf (Warne, Webb, and Larsen 2005).

4.5 Pearson correlation of Kd490 and [Chla] with river discharge at 2km from the river mouth and along the shelf

The maximum range for [Chla] and Kd490 values for all the four regions were highest near the river mouth for the rainy and dry seasons (*i.e.*, at 2km away). This maximal range decreased along the insular shelf. It can be expected that the spreading of sediments be distributed mostly along insular shelves and coastal regions (Brown *et al.*, 2008). Therefore, from the rivers to the open ocean, finer clay material can travel via suspension and resuspension to the deep ocean floor. Biogenic sediments are the main constituents of the deep ocean pelagic sediments because they float (*op. cit.*). These authors also stated that, the larger the grain size, the slower the flow, whereas the smaller the grain sediment, the faster the flow and the higher the suspension and resuspension. As a result, sediment movement in the shallow waters occurs in the entire water column, whereas in the deeper waters it occurs mostly at the benthos (Brown *et al.*, 2008).

Even though high river discharge has been usually perceived to be directly proportional to high turbidity in coastal waters, this was the case only for the Eastern region. It could be due to the fact that the influence of river discharge on [Chla] and Kd490 was intensified along, and slowly dissipating with distance. To the contrary, the Western region turbidity was inversely proportional to river discharge, away from 2km. This was likely due to the fact that the influence of river discharge on [Chla] and Kd490 was rapidly and continuously dissipated with distance. Based on the findings of Morelock *et al.* (2000), these results could be explained by the various regional shelf morphologies of Puerto Rico. It could also be due to the fact that the river discharge stations were not exactly at the river mouths, causing a lag time in the river discharge. It could be from any combination of the regional characteristics previously discussed in this section.

The fact that [Chla] *r* was better correlated to river discharge than to Kd490, as discussed in the previous section, could be due to the fact that turbidity was more influenced by biogenic particles than non-biogenic particles (*i.e.*, terrigenous sediments) in relation to river discharge in coastal waters of Puerto Rico from 1998 to 2013.

In relation to river discharge, as mentioned earlier, in the insular shelf, dry season [Chla] and Kd490 *r* were better correlated to river discharge than to rainy season, but for the Northern rivers (narrower insular shelf in comparison with the other regions), could be due to winter frontal storms having more impacts on the entire shelf, in comparison to hurricanes and similar events affecting, for the most part, the inner and middle shelf (Warne, Webb, and Larsen 2005).

5 CONCLUSIONS

Chlorophyll *a* concentration was the main contributor to turbidity in coastal waters of Puerto Rico during 1998 to 2013. In addition, there were regional and seasonal variability trends in chlorophyll *a* concentration, diffuse vertical attenuation coefficient for downward irradiance at 490nm, and river discharge. Moreover, in the annual and rainy season trends, turbidity had increased in the Western region, whereas, it had decreased in the dry season. To the contrary, in the annual and rainy season trends, turbidity had decreased in the Northern region, whereas, it had increased in the dry season. In the annual and seasonal trends, turbidity had decreased. Also, in the Eastern region, turbidity was strongly influenced by river discharge. On the contrary, in the Western region, turbidity was weakly controlled by river discharge.

The hypotheses had been either partially or fully accepted. The first hypothesis: “There was a decreasing trend in Kd490 and [Chla] in the coastal waters of Puerto Rico from 1998 to 2013”, has been rejected for the annual and rainy season for the West region, for the dry season for the Northern region, and for the Eastern region for Kd490 only. It was accepted for the annual and rainy season for the Northern, Eastern, and Southern regions, as well as for the dry season for the Western and Southern regions, and for the Eastern region [Chla] only. The second hypothesis: “Seasonal and regional patterns of [Chla] in coastal waters were correlated with Kd490” has been accepted for all the seasons and for all the regions. The third hypothesis: “Seasonal and regional patterns in Kd490 in coastal regions were directly proportional to the river discharge” has been rejected for the annual, rainy and dry seasons for the Southern region, for the annual and rainy season for the Eastern region, as well as for the dry season for the Northern region. It has been accepted for all the seasons for the Western region, for the dry season for the Eastern region, and for the annual and rainy season for the Northern region. It was statistically significant for the annual and dry season for the Eastern region. The fourth hypothesis: “[Chla] concentration in coastal areas was directly proportional to seasonal and regional patterns of river discharge” has been rejected for the annual, rainy and dry seasons for the Southern region, for the rainy season for the Eastern region, as well as for the dry season for the Northern region. It has been accepted for all the seasons for the Western region, for the annual and dry season for the Eastern region, as well as for the annual and rainy season for the Northern region. It was statistically significant for the annual and dry season for the Eastern region.

There were some limitations to this study. The trends and correlations were based on a 16-year relative to the high rainfall episode of Hurricane Georges in 1998, which was the major episodic event that affected Puerto Rico during the last decades. Other limitations could be from the spatial and temporal resolution of the data. Higher temporal and spatial resolution data might be more appropriate but the files would be bigger, more time processing would be required, which would be more costly. Furthermore, incorporating *in situ* data from ships and other methods would be beneficial to validate the satellite data. The river stations were not exactly at the river mouth, introducing a lag time in river discharge. The river discharge data could also have been influenced by other factors, such as land cover and land use (*e.g.*, urban, rural, agricultural, forested, industrial).

This is the first time that 16 years of daily data of chlorophyll *a* concentration, diffuse vertical attenuation coefficient for downward irradiance at 490nm were processed, and combined with river discharge data for coastal waters of Puerto Rico. My principal conclusion is that chlorophyll *a* concentration (*i.e.*, biogenic sediments) and not non-biogenic sediments (*i.e.*, terrigenous sediments) was the primordial factor determining turbidity in coastal waters of Puerto Rico for that 16-year time period.

This study could be used as a baseline for other research. For instance, to assess the influence of terrigenous sediments to turbidity and in comparison with [Chla] during specific episodic rainfall events in coastal waters of Puerto Rico.

From a management perspective, this study could be used as a baseline for seasonally and regionally monitoring [Chla] and Kd490 for optimal conditions for the sustainability of the marine ecosystem, such as the benthic community, by evaluating the effects of the quantity and frequency of rainfall episodic events in the coastal waters of Puerto Rico. Increasing trends of turbidity, mainly by [Chla], would be beneficial at optimal levels to benthic habitats such as coral reefs and other benthos by providing nutrients and protection against UV rays. However, it would be detrimental, if the [Chla] levels were very elevated, causing eutrophication and resulting to harmful algal blooms, and algal shift population, which could deplete oxygen and other factors necessary for benthic communities to thrive.

6 LITERATURE CITED

Abal, E.G. and Dennison, W.C., 1996. Seagrass depth range and water quality in southern Moreton Bay, Queensland, Australia. *Marine Freshwater Research,* 47, 763–771.

Ahmad, R.; Scatena, F.N., and Gupta, A., 1993. Morphology and sedimentation in Caribbean mountain streams: examples from Jamaica and Puerto Rico. *Sedimentary Geology,* 85, 157-169.

Ballantine, D. L.; Appeldoorn, R.S.; Yoshioka P.; Weil, E.; Armstrong, R.; García, J.R.; Otero, E.; Pagan, F.; Sherman, C., and Hernandez-Delgado, E.A., 2008. Biology and Ecology of Puerto Rican Coral Reefs, Coral Reefs of the USA. *In*: Riegl, B.M and Dodge, R.E. (eds.), *Coral Reefs of the World*. The Netherlands: Springer, pp. 375-406.

Baith, K.; Lindsay, R.; Fu, G., and McClain, C.R., 2001. SeaDAS, a data analysis system for ocean-color satellite sensors. *EOS, Transactions, American Geophysical Union,* 82(18), 202.

Bierwirth, P.N.; Lee, T.J., and Burne, R.V., 1993. Shallow sea-floor reflectance and water depth derived by unmixing multispectral imagery. *Photogrammetric Engineering and Remote Sensing*, 59, 331–38.

Brown, E.; Colling, A.; Park, D.; Phillips, J.; Rothery, D., and Wright, J., 2007. The Atmosphere and the Ocean. *In*: Colling, A. (ed.), *Ocean Circulation*. Burlington, Massachusetts, USA: Butterworth-Heinemann, pp. 18-31.

Brown, E.; Colling, A.; Park, D.; Phillips, J.; Rothery, D., and Wright, J., 2007. Other Major Currents. *In*: Colling, A. (ed.), *Ocean Circulation*. Burlington, Massachusetts, USA: Butterworth-Heinemann, pp. 170-176.

Brown, E.; Colling, A.; Park, D.; Phillips, J.; Rothery, D., and Wright, J., 2008. Introduction to Shallow-Water Environments and their Sediments. *In*: Park, D. (ed.), *Waves, Tides and Shallow-Water Processes*. Burlington, Massachusetts, USA: Butterworth-Heinemann, pp. 87-95.

Brown, E.; Colling, A.; Park, D.; Phillips, J.; Rothery, D., and Wright, J., 2008. Principles and Processes of Sediment Transport. *In*: Park, D. (ed.), *Waves, Tides and Shallow-Water Processes*. Burlington, Massachusetts, USA: Butterworth-Heinemann, pp. 96-124.

Carder, K.L.; Chen, F.R.; Lee, Z.P.; Hawes, S.K., and Kamykowski, D., 1999. Semianalytic moderate-resolution imaging spectrometer algorithms for chlorophyll-a and absorption with bio-optical domains based on nitrate depletion temperatures. *Journal of Geophysical Research,* 104, 5403-5421.

Catts, G.P.; Khorram, S.; Cloern, J.E.; Knight, A.W., and DeGloria, S.D., 1985. Remote sensing of tidal chlorophyll-a variations in estuaries. *International Journal of Remote Sensing*, 11, 1685–706.

Dekker, A.G.; Zamurovic-Nenad, Z.; Hoogenboom, H.J., and Peters, S.W.M., 1996. Remote sensing, ecological water quality modelling and in situ measurements: a case study in shallow lakes. *Journal des Sciences Hydrologiques,* 41, 531–47.

Díaz, P.L.; Aquino, Z.; Figueroa-Alamo, C.; Vachier, R. J., and Sánchez, A.V., 1998. *Water resources data Puerto Rico and the U.S. Virgin Islands water year 1998: U.S. Geological Survey Water-Data Report PR-98-1*, 631 p.

Esaias, W. E.; Abbott, M. R.; Barton, I.; Brown, O. B.; Campbell, J.W.; Carder, K. L.; Clark, D.K.; Evans, R. H.; Hoge, F. E.; Gordon, H. R.; Balch, W. M.; Letelier, R., and Minnett, P.

J., 1998. An overview of MODIS capabilities for ocean science observations. *IEEE Transactions of Geoscience Remote Sensing*, 36(4), 1250–1265.

Feldman, G. C., C. R. McClain, Ocean Color Data Browsers level 1 & 2,Ocean Color Web, Eds. Kuring, N., Bailey, S. W., Franz, B. A., Meister, G., Werdell, P. J., Eplee, R. E.,. NASA Goddard Space Flight Center. 2014. *http://oceancolor.gsfc.nasa.gov/cgi/browse.pl?sen=am.*

Feldman, G. C. and McClain, C. R., 2014. *An Overview of SeaWiFS and the SeaStar Spacecraft, Ocean Color Web*. NASA Goddard Space Flight Center. *In*: Kuring, N.; Bailey, S. W.; Franz, B. A.; Meister, G.; Werdell, P. J., and Eplee, R. E. (eds.). *http://oceancolor.gsfc.nasa.gov/SeaWiFS/SEASTAR/SPACECRAFT.html*.

Feldman, G. C. and McClain, C. R., 2014. *Ocean Color Web, Product Level Descriptions, Ocean Color Web*. NASA Goddard Space Flight Center. *In*: Kuring, N.; Bailey, S. W.; Franz, B. A.; Meister, G.; Werdell, P. J., and Eplee, R. E. (eds.). *http://oceancolor.gsfc.nasa.gov/cms/products*.

Feldman, G. C. and McClain, C. R., 2014. *Ocean Color Web, SeaWiFS Reprocessing 2014.0*. NASA Goddard Space Flight Center. *In*: Kuring, N. and Bailey, S. W. (eds.). 05-2014. *http://oceancolor.gsfc.nasa.gov/cms/reprocessing/OCReproc20140SW.html*.

Feldman, G. C. and McClain, C. R., 2014. *Ocean Color Web, MODIS Aqua Reprocessing 2013.1*, NASA Goddard Space Flight Center. *In*: Kuring, N. and Bailey, S. W. (eds.). 05-2014. *http://oceancolor.gsfc.nasa.gov/cms/reprocessing/OCReproc20131MA.html*.

Fieldler, P.C. and Laurs, R.M., 1990. Variability of the Columbia River plume observed in visible and infrared satellite imagery. *International Journal of Remote Sensing*, 11, 999–1010.

Frazier, S. and Maccherone, B., 2014. *MODIS Web, About MODIS, NASA. https://modis.gsfc.nasa.gov/about/*.

Frazier, S. and Maccherone, B., 2014. *MODIS Web, About MODIS, NASA. https://modis.gsfc.nasa.gov/about/specifications.php*.

García-Sais, J.; Williams, S., and Amirrezvani, A., (in review). Recuperation and phase shifts of scleractinian coral assemblages on Puertorrican coral reefs one decade after the 2005 regional coral bleaching event. *Marine Ecology Progress Series*.

Gilbes, F.; López, J.M., and Yoshioka, P.M., 1996. Spatial and Temporal Variations of Phytoplankton Chlorophyll-a and Suspended Particulate Matter in Mayagüez Bay, Puerto Rico. *Journal of Plankton Research*, 18(1), 29-43.

Gilbes, F.; Armstrong, R.A.; Webb, R.M.T, and Müller-Karger, F., 2001. SeaWiFS helps assess hurricane impact on phytoplankton in Caribbean Sea. *EOS, Transactions American Geophysical Union*, 529-533.

Gordon, H.R. and Morel, A., 1983. *Remote assessment of ocean color for interpretation of satellite visible imagery. A review*. New York, New York, USA: Springer-Verlag New York, 114p.

Gupta, A., 1988. Large floods as geomorphic events in the humid tropics. *In*: Baker, V.R.; Kochel, R.C., and Patton, P.C. (eds.), *Flood Geomorphology*. New York: John Wiley, pp. 301-314.

Gupta, A., 2000. Hurricane floods as extreme geomorphic events. *In*: Hasan, M.A.; Slaymaker, O., and Berkowicz, S.M. (eds.), *The Hydrology-Geomorphology Interface: Rainfall, Floods,* *Sedimentation, Land Use, Proceedings of the International Association of Hydrological Sciences* (Jerusalem, Israel), 261, 215-228.

Ho, F.P., 1975. *Storm-tide frequency analysis for the coast of Puerto Rico*. Silver Spring, Maryland: National Weather Service, National Oceanic and Atmospheric Administration, *Technical Memorandum NWS HYDRO-23*, 43 p.

Hooker, S. B.; Esaias, W. E.; Feldman, G. C.; Gregg, W. W., and McClain, C. R., 1992. *An overview of SeaWiFS and ocean color*. Greenbelt, Maryland: NASA Goddard Space Flight Center. *In*: Hooker, S. B. and Firestone, E. R. (eds.), *NASA Technical Memorandum 104566*, (1), 24 p., plus color plates.

Hu, C.; Lee, Z., and Franz, B.A., 2012. Chlorophyll-a algorithms for oligotrophic oceans: A novel approach based on three-band reflectance difference. *Journal of Geophysical Research*, 117, C01011. doi:10.1029/2011JC007395.

Johnson, R.W. and Harriss, R.C., 1980. Remote sensing for water quality and biological measurements in coastal waters. *Photogrammetric Engineering and Remote Sensing*, 46, 77–85.

Katwijk, M.M.; Meier, N.F.; van Loon, R.; van Hove, E.M.; Giesen, W.B.J.T.; van der Velde, G., and den Hartog, C., 1993. Sabaki River sediment load and coral stress: correlation between sediments and condition of the Malindi-Watamu reefs in Kenya (Indian Ocean). *Marine Biology*, 117, 675-683.

Khorram, S.; Cheshire, H.; Geraci, A., and Rosa, G.L., 1991. Water quality mapping of Augusta Bay, Italy from Landsat TM data. *International Journal of Remote Sensing*, 12, 803–808.

Kirk, J. T. O., 2011. *Light and photosynthesis in aquatic ecosystems.* Cambridge: Cambridge University Press, 662p.

Kleypas, J.A., 1996. Coral reef development under naturally turbid conditions: fringing reefs near Broad Sound, Australia. *Coral Reefs*, 15, 153–167.

Larcombe, P.; Ridd, P.V.; Prytz, A., and Wilson, B., 1995. Factors controlling suspended sediment on inner-shelf coral reefs, Townsville, Australia. *Coral Reefs*, 14, 163–171.

Maritorena, S. and O'Reilly, J. E., 2000. *OC2v2: Update on the Initial Operational SeaWiFS Chlorophyll a Algorithm.* Greenbelt, Maryland: NASA Goddard Space Flight Center. *In*: Hooker, S. B. and Firestone, E. R. (eds.), *NASA Technical Memorandum 2000-206892, (*11), pp. 3-8. http://oceancolor.gsfc.nasa.gov/cgi/postlaunch_tech_memo.pl?11.

MATLAB version 7.12.0 Natick, Massachusetts: The MathWorks Inc., 2011.

McClain, C. R.; Cleave, M. L.; Feldman, G. C.; Gregg, W.W.; Hooker, S. B., and Kuring, N., 1998. Science quality SeaWiFS data for global biosphere research. *Sea Technology*, 39, 10-16.

McKergow, L.A.; Prosser, I.P.; Hughes, A.O., and Brodie, J., 2005. Regional scale nutrient modeling: exports to the Great Barrier Reef world heritage area. *Marine Pollution Bulletin*, 51, 186–199.

Miller, R. L.; Cruise, J. F.; Otero, E., and López, J. M., 1994. Monitoring suspended particulate matter in Puerto Rico: field measurements and remote sensing. *Water Research Bulletin*, 30(2), 271-282.

Miller, R. L. and Cruise, J. F., 1995. Effects of suspended sediments on coral growth: Evidence from remote sensing and hydrologic modeling. *Remote Sensing Environment*, 53, 177–187.

Miller, R. L. and McKee, B. A., 2004. Using MODIS Terra 250 m imagery to map concentrations of total suspended matter in coastal waters. *Remote Sensing of Environment*, 93, 259–266.

Morelock, J.; Capella, J.; Garcia, J.R., and Barreto, M., 2000. Puerto Rico - Seas at the Millennium. *In*: Sheppard, C.R.C. (ed.), *Seas at the Millennium*. London, England: Oxford Press, 13p.

Morelock, J.; Wilson, R.; Bruckner, A.; Carlo, M., and Mayor, P., 2001. Status of coral reefs, southwest Puerto Rico. *Caribbean Journal of Science Special Publication*, (4), 57 p.

Neuman, C.J.; Jarvinen B.R. and Pike, A.C., 1990. *Tropical cyclones of the North Atlantic Ocean, 1871-1986 (with storms tracks updated through 1989). National Climatic Data Center Historical Climatology Series 6-2*, 186 p.

National Oceanic and Atmospheric Administration, National Hurricane Center. Atlantic Hurricane Seasons. http://www.nhc.noaa.gov/data/tcr/index.php?basin=atl.

National Oceanic and Atmospheric Administration, National Weather Service, Climate Prediction Center. Cold and Warm Episodes by Season. http://www.cpc.noaa.gov/products/analysis_monitoring/ensostuff/ensoyears.shtml.

O'Reilly, J.E.; Maritorena, S.; Mitchell, B.G.; Siegel, D.A.; Carder, K.L.; Garver, S.A.; Kahru, M., and McClain, C., 1998. Ocean color chlorophyll algorithms for SeaWiFS. *Journal of Geophysical Research*, (103), 24.937-24.953.

O'Reilly J.E.; Maritorena S.; Siegel D.; O'Brien M.; Toole D.T.; Mitchell B.G.; Kahru M.; Chavez F.P.; Strutton P.; Cota G.F.; Hooker S.B.; McClain C.R.; Carder K.L.; Muller-Karger F.E.; Harding L.; Magnuson A.; Phinney D.; Moore G.F.; Aiken J.; Arrigo K.R.; Letelier, R.M., and Culver, M.E., 2000. *Ocean Color Chlorophyll a algorithms for SeaWiFS, OC2 and OC4: Version 4. SeaWiFS Postlaunch Calibration and Validation Analyses, Part 3*. Greenbelt, Maryland: NASA Goddard Space Flight Center. *In*: Hooker, S. B. and Firestone, E. R. (eds.), *NASA Technical Memorandum 2000-206892, (*11), pp. 9-23. http://oceancolor.gsfc.nasa.gov/cgi/postlaunch_tech_memo.pl?11.

Scatena, F.N. and Larsen, M.C., 1991. Physical aspects of Hurricane Hugo in Puerto Rico. *Biotropica*, 23(4a), 317-323.

Sheng J.; Wang, L.; Andréfouët, S.; Hu, C.; Hatcher, B.G.; Muller-Karger, F.E.; B. Kjerfe; Heymans, W.D., and Yang, B., 2007. Upper ocean response of the Mesoamerican barrier reef system to hurricane Mitch and coastal freshwater inputs: a study using SeaWiFS ocean color data and a nested-grid ocean circulation model. *Journal of Geophysical Research*, 112, C07016, 22p.

Soler-López, L.R., 2001. Sedimentation survey results of the principal water-supply reservoirs of Puerto Rico. *In*: Sylva, W.F. (ed.), *Proceedings of the Sixth Caribbean Islands Water Resources Congress* (Mayagüez, Puerto Rico), unpaginated cd.

Torres-Sierra, H., 1996. *Flood of January 5-6, 1992, in Puerto Rico. U.S. Geological Survey Open-File Report*, pp. 95-374, 13 p.

USGS, USGS Surface-Water data for USA. http://waterdata.usgs.gov/pr/nwis/sw.

USGS, Annual Water Data Report. http://wdr.water.usgs.gov/allsearch.php#sw.

Walker, N.D., 1996. Satellite assessment of Mississippi River plume variability: causes and predictability. *Remote Sensing of Environment*, 58, 21–35.

Warne, A.G.; Webb, R.M.T., and Larsen, M.C., 2005. *Water, sediment, and nutrient discharge characteristics of rivers in Puerto Rico, and their potential influence on coral reefs. U.S. Geological Survey Scientific Investigations Report. 2005-5206*, 58 p.

Wilkinson, C.R., 1999. Global and local threats to coral reef functioning and existence: review and predictions. *Marine Freshwater Research,* 50, 867–878.